Tribol Lett (2010) 40:375–394
DOI 10.1007/s11249-010-9659-4

ORIGINAL PAPER

# Substituent Effect on the Reactivity of Alkylated Triphenyl Phosphorothionates in Oil Solution in the Presence of Iron Particles

**Filippo Mangolini · Antonella Rossi · Nicholas D. Spencer**

Received: 29 May 2010 / Accepted: 7 July 2010 / Published online: 30 July 2010


**Abstract** The effect of the substituent attached to the phenyl rings on the reactivity of alkylated triphenyl phosphorothionates (*t*-butyl TPPT (b-TPPT) and *p*-nonyl TPPT (n-TPPT)) in oil solution at high temperature (423 and 473 K) was investigated by means of Fourier-transform infrared spectroscopy (FT-IR), nuclear magnetic resonance (NMR) spectroscopy and X-ray photoelectron spectroscopy (XPS). The FT-IR and NMR results show that the alkylated TPPTs were highly thermally stable and did not completely decompose in oil, even upon heating at 423 K for 168 h and at 473 K for 72 h, with and without steel filings and iron particles (both metallic iron and iron oxide particles). The reaction of alkylated TPPTs was found to start with the scission of the P=S bond to yield alkylated triphenyl phosphate. The kinetics of the thermo-oxidative reaction was slower when steel filings and iron particles were added to the oil solutions during the heating experiments. The reactivity of the unsubstituted molecule (TPPT) was higher than that of alkylated TPPTs at 423 K, while at 473 K TPPT and n-TPPT were more reactive than b-TPPT. In the case of the experiments performed at 473 K in the presence of steel filings or metallic iron or iron oxide particles, the reactivity of the alkylated TPPT molecules decreased with the length of the alkyl chain bound to the phenyl rings. The XPS results show that a reaction layer consisting of carbon, oxygen, phosphorus and iron was formed on the 100Cr6 steel filings immersed for 72 h in oil solutions containing alkylated TPPTs and heated at 473 K. Sulphur was neither detected on the surface nor in the composition vs depth profile. During the heating experiments, the base oil (PAO) was oxidized. At 423 K, the alkylated TPPTs had a strong antioxidant effect, which was found to be more pronounced upon increasing the length of the alkyl chain bound to the phenyl rings. At 473 K, the TPPTs did not inhibit the oxidation of the base oil as effectively as at 423 K.

**Keywords** Thermo-oxidative degradation · *t*-butyl triphenyl phosphorothionate (b-TPPT) · Irgalube® 232 · *p*-nonyl triphenyl phosphorothionate (n-TPPT) · Irgalube® 211 · Ashless anti-wear additives · Low-SAPS additives · FT-IR · NMR · XPS · Iron particles

## 1 Introduction

The development of exhaust after-treatment systems for gasoline and diesel automobile engines over the last 20 years has brought about a need to change the engine-lubricant composition, in order to minimize the degradation of catalysts and filters over the operating life of an engine. Three main components of engine lubricant additives, i.e. phosphorus, sulphur and metals, have been demonstrated to lead to a loss of emission-control catalyst effectiveness and to block filters within the exhaust after-treatment system [1]. Consequently, modern engine-lubricant specifications are progressively limiting the permissible levels of sulphated ash, phosphorus and sulphur (SAPS) in oil formulations [2].

F. Mangolini · A. Rossi · N. D. Spencer (✉)
Department of Materials, ETH Zurich, Laboratory for Surface Science and Technology, Wolfgang-Pauli-Strasse 10, 8093 Zurich, Switzerland
e-mail: nspencer@ethz.ch

A. Rossi
Dipartimento di Chimica Inorganica ed Analitica, Università degli Studi di Cagliari, INSTM unit - Cittadella Universitaria di Monserrato, 09100 Cagliari, Italy

Among the many additives that are employed for formulating engine lubricants, zinc dialkyldithiophosphates (ZnDTP) probably represent one of the most successful class of compounds ever synthesized. First introduced as antioxidants in the 1940s (they act as both primary (i.e. radical trapping) and secondary (i.e. peroxide-decomposing) antioxidants), it soon became clear that ZnDTPs also combine good antiwear and extreme-pressure properties [2–9]. The performance of ZnDTPs is strongly influenced by the chemical structure of the molecule, which mainly depends on the type of alcohols used for the synthesis [8]. Moving from primary alkyl to secondary alkyl ZnDTPs, the oxidative inhibition and wear protection performance improves, while the thermal stability decreases. This structure-activity dependence of ZnDTPs was explained by the ease with which the nucleophilic substitution at the α-carbon atom of the alkyl group can take place [10]. Compared to the alkyl varieties, aryl ZnDTPs usually show inferior antioxidant and antiwear performance, but superior thermal stability [8].

In spite of the remarkable effectiveness of ZnDTPs over a wide range of conditions, the large amounts of all three catalyst-poisoning agents (phosphorus, sulphur and zinc) present in this class of compounds brought environmental considerations of their use in engine oils into focus. Although the concentration of ZnDTPs in lubricant formulation has already been reduced [11], the development of new additives with lower- or zero-SAPS levels is becoming a necessity [12, 13].

Among the different chemistries that have been proposed as replacement or supplement to ZnDTPs in engine oils, ashless equivalents to ZnDTPs, i.e. thiophosphates and phosphates without any metal, have already been investigated quite extensively. In the last decade, the antiwear performance as well as the nature and properties of the films formed on tribological surfaces by these new environmentally friendly additives have been studied by several research groups [12].

Hilgetag and Teichmann [14, 15] described the chemical behaviour of pure organophosphates and organothiophosphates, focusing, in particular, on the difference in the nucleophilic reactivities of the phosphoryl and thiophosphoryl groups. The key chemical feature of these classes of compounds is their strong alkylating power. All the reactions were explained on the basis of Pearson's acid–base concept [16–19], according to which oxygen is a "hard base" and preferentially reacts with "hard acids", such as protons, "A" metals (alkali metal cations, transition metal cations in high oxidation states), carbonyl carbon and phosphoryl phosphorus. In contrast, sulphur is a "soft base" and mainly reacts with "soft acids", such as "B" metals (transition metal cations in low oxidation states), tetrahedral carbon and halogens.

The reactivity of tributyl thiophosphate (TBT) with air-oxidized iron surfaces at 373 K has been investigated by in situ attenuated total reflection (ATR/FT-IR) tribometry, X-ray photoelectron spectroscopy (XPS) and temperature-programmed reaction spectroscopy (TPRS) [20]. Thermal films and tribofilms were found to consist of iron polyphosphate and sulphate. Compared to the reaction layers generated under purely thermal conditions, the amount of sulphate and polyphosphate was higher in the films formed under tribological conditions in the boundary-lubrication regime. The comparison of the surface chemistry of TBT with that of tributyl phosphate (TBP) allowed the authors to clarify the role of sulphur in this class of molecules: it facilitates the formation of long-chain polyphosphates and lowers the temperature of the chemical and tribochemical reactions by around 50 K.

The study of the chemical reactions occurring in oil at high temperature could provide an insight into the mechanism of thermal film and tribofilm formation as well as into the antioxidant properties of an additive, as demonstrated in the case of ZnDTPs [4, 6]. For this reason, the reactivity of triphenyl phosphorothionate (TPPT) in synthetic oil (poly-α-olefin, PAO) at 423 and 473 K has been recently investigated in our group by Fourier-transform infrared spectroscopy (FT-IR) and nuclear magnetic resonance (NMR) spectroscopy [21]. The FT-IR and NMR results showed that this molecule possesses high thermal stability in lubricant oil solution. A thermo-oxidative reaction was found to start with the scission of the P=S bond and to result in the formation of triphenyl phosphate (TPP). The oxidation of the base oil, which involves a four-step free-radical reaction (initiation of the radical chain reaction, chain propagation, chain branching and termination of the radical chain reaction), leading to the formation of a complex mixture of oxygenated products (e.g. hydroperoxides, alkyl peroxides, alcohols, carboxylic acids, peroxy acids, esters, ketones, aldehydes and lactones) [8, 22, 23], also suggested that the TPPT molecule is not an effective oxidation inhibitor, in contrast to ZnDTPs.

The presence of metallic or oxidized iron particles in the oil solution during the heating experiments was shown to catalyze the reaction of TPPT to yield TPP, but not to change the reaction mechanism [24]. However, the concentration of TPP in oil solution generated by the thermo-oxidative reaction of TPPT was lower when the heating experiments were carried out in the presence of metallic and oxidized iron particles. The XPS results showed that a reaction layer was formed on the 100Cr6 steel filings immersed for 72 h in TPPT solution heated at 473 K and was found to consist of carbon, oxygen, phosphorus and iron. The XPS sputtering depth profile revealed the presence of sulphur in the reaction layer, starting from a

sputtering depth of 3.5 ± 0.1 nm relative to a $Si/SiO_2$ reference sample.

The surface reactivity of alkylated phosphorothionates (triphenyl phosphorothionates (TPPTs) substituted with alkyl chains of different lengths) with air-oxidized steel was also investigated in our group [25, 26]. The activation temperature for the thermal decomposition of TPPTs was found to be around 423 K. At 423 K a thin reaction layer, consisting of short-chain polyphosphates and oxidized sulphur species, was formed in the non-contact region of air-oxidized steel (thickness of the oxide layer: 2.7 ± 0.2 nm) after ca. 5 h, as indicated by the XPS results. The composition of the layer generated at 423 K was found to be dependent on the length of the alkyl chains bound to the phenyl rings: with longer chains, the phosphate concentration decreased, while the sulphur concentration increased. On the basis of these findings, a reaction mechanism was proposed: following the adsorption of the sulphur atom to the surface, as suggested by Koyama et al. [27], the phosphorothionate molecules started decomposing with the scission of the P=S bond, followed by the cleavage of the C–O or P–O bond. The released sulphur was then oxidized.

To the knowledge of the authors, no systematic study of the effect of the substituent attached to the phenyl ring in triphenyl phosphorothionate or phosphate on the reactivity in oil solution has ever been carried out. The substitution of the phenyl ring with alkyl chains is usually made in order to enhance the solubility of the molecules in oil [28].

In the present work, the effect of the substituent bound to the phenyl ring of triphenyl phosphorothionates (*t*-butyl TPPT (b-TPPT) and *p*-nonyl TPPT (n-TPPT)) on the reactivity of these molecules in synthetic oil (poly-α-olefin) at high temperature (423 and 473 K) has been investigated for the first time by means of FT-IR and NMR spectroscopy. The surface chemistry of the 100Cr6 steel filings immersed in the heated oil solutions (473 K for 72 h) has been studied by XPS sputter depth profiling. A comparison with the results presented in our previous work and obtained using the unsubstituted molecule (i.e. TPPT) [21, 24] has also been performed.

## 2 Experimental

### 2.1 Materials

Poly-α-olefin (PAO, Durasyn® 166, Tunap Industrie GmbH & Co., Mississauga, Canada) was used as base oil and blended with *t*-butyl TPPT (b-TPPT, Irgalube® 232, Ciba Speciality Chemicals, Basel, Switzerland) and *p*-nonyl TPPT (n-TPPT, Irgalube® 211, Ciba Speciality Chemicals, Basel, Switzerland) (Fig. 1). The purification of the lubricant additives was carried out by liquid chromatography.

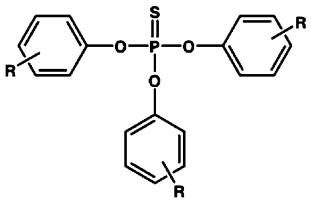


**Fig. 1** Chemical formula of alkylated triphenyl phosphorothionates (TPPTs). The alkyl chain R is *t*-butyl (b-TPPT) or *p*-nonyl (n-TPPT)

For the heating experiments, a 0.068 mol $dm^{-3}$ (4.2 wt.%) solution of b-TPPT in PAO and a 0.043 mol $dm^{-3}$ (3.77 wt.%) solution of n-TPPT in PAO were prepared. For dissolving the b-TPPT and the n-TPPT in the base oil, an ultrasonic bath was employed for four cycles of 10 min each. The temperature of the lubricant solution was always maintained below 318 K during the ultrasonic treatment.

In order to investigate the influence of metallic and oxidized iron/steel on the reactivity of alkylated TPPTs in oil solution, either 100Cr6 steel (AISI 52100) filings or metallic iron (Fluka, purum, reduced, ≥99.0% (RT), powder) or iron oxide particles were added to the lubricant oil solutions during the heating experiments. The iron oxide was prepared from (Fluka, purum, reduced, ≥99.0% (RT)) iron powder oxidized at 573 K for 3 h in $Al_2O_3$ crucibles (Metoxit AG, Thayngen, Switzerland)). In the following text, the metallic iron and iron oxide particles will be referred to as $Fe_{part}$ and $FeOx_{part}$, respectively. The specific surface area of the 100Cr6 steel filings and of the metallic/oxidized iron particles was determined by $N_2$ adsorption using the Brunauer, Emmett and Teller (BET) method and found to be 0.19 ± 0.01 $m^2$ $g^{-1}$ and 0.07 ± 0.04 $m^2$ $g^{-1}$, respectively [24]. The characterization of the surface chemistry of the as-received 100Cr6 steel filings, metallic iron and iron oxide particles by XPS is described in [24].

The vacuum filtration of the solutions at the end of the experiments was carried out using cellulose filter papers with 2.5 μm particle retention in liquid (Grade 42, Whatman®, Maidstone, England).

### 2.2 Methods

#### *2.2.1 Heating Experiments*

The heating experiments were performed by immersing a glass flask (40 $cm^3$, 95 × 27.5 $mm^2$, VWR International, Dietikon, Switzerland) containing 15 $cm^3$ of the lubricant solution in a silicone oil bath that was heated at 423 K and at 473 K (±1 K). In order to investigate the influence of metallic and oxidized iron/steel on the reactivity of alkylated TPPTs in oil solution, 1.25 ± 0.01 g of 100Cr6 steel

filings or $Fe_{part}$ or $FeOx_{part}$ was added to the oil solutions. During the experiment the solution, open to air, was neither stirred nor purged with any gas. The duration of the heating varied between 3 and 168 h at 423 K and between 3 and 72 h at 473 K. The relative humidity was maintained between 22 and 30%.

After the test, the glass flask was removed from the silicone oil bath and left for 45 min in air to cool down without any cover. The solution was then vacuum filtered in order to remove any precipitates formed and the added 100Cr6 steel filings, $Fe_{part}$ and $FeOx_{part}$.

### 2.2.2 Microelemental Analysis

The microelemental analysis was carried out using a CHN-900 (Leco Corporation, Michigan, USA) for carbon and hydrogen, a CHNS-932 (Leco Corporation, Michigan, USA) for sulphur and a RO-478 (Leco Corporation, Michigan, USA) for oxygen. The phosphorus content was determined by the molybdovanadate method [29] after microwave digestion and leaching ($2 \times 50$ min) in concentrated sulphuric acid and perchloric acid at 483–508 K.

### 2.2.3 Fourier Transform Infrared Spectroscopy (FT-IR)

Transmission FT-IR spectra were acquired with a Nicolet™ 5700 Fourier Transform Infrared spectrometer (Thermo Electron Corporation, Madison, WI, USA). The experimental conditions are listed in Table 1. Sampling was performed by placing one drop of solution onto a KBr pellet.

The spectra were processed with OMNIC™ software (V7.2, Thermo Electron Corporation, Madison, WI, USA). A single-beam spectrum of the KBr pellet was acquired before each measurement as a background. Normalization was carried out with respect to the methyl asymmetric deformation band, overlapped by the methylene scissor vibration band of PAO at 1466 $cm^{-1}$ [30].

### 2.2.4 Nuclear Magnetic Resonance (NMR) Spectroscopy

The NMR spectra were recorded in $CDCl_3$ (99.8 at.% D, Armar Chemicals, Döttingen, Switzerland) at 300 K using a Bruker Avance 500 NMR spectrometer operating at 500.1 (1-H), 125.8 (13-C) and 202.5 (31-P) MHz. The chemical shifts, given as dimensionless values, were referred to TMS (1-H and 13-C) and $H_3PO_4$ (85%) following the IUPAC recommendation [31].

**Table 1** Transmission FT-IR experimental conditions

| Detector | DGTS/KBr |
|---|---|
| Resolution | 2 $cm^{-1}$ |
| Number of scans | 64 |
| Scan velocity | 0.6329 cm/s |
| Acquisition time | 136 s |
| Gain control | 1 |

### 2.2.5 X-ray Photoelectron Spectroscopy (XPS)

The depth distribution of the elements present in the reaction layer formed on the 100Cr6 steel filings immersed in a 0.068 mol $dm^{-3}$ solution of b-TPPT in PAO or in a 0.043 mol $dm^{-3}$ solution of n-TPPT in PAO heated at 473 K for 72 h was determined by XPS sputter depth profiling.

The XPS analyses were carried out using a PHI Quantera SXM (ULVAC-PHI, Chanhassen, MN, USA) spectrometer. The X-ray source of the PHI Quantera SXM is a focused and scanned monochromatic Al Kα with beam diameters between 9 and 200 μm. The emitted electrons are collected and retarded with a Gauze lens system at an emission angle (EA) of 45°. After passing the hemispherical analyzer, the electrons are detected in a 32-channel detector. The system is equipped with a high-performance, floating-column ion gun and an electron neutralizer for charge control and correction. The points to be analysed were chosen using optical microscopic images in combination with X-ray induced secondary electron images (SXI). The residual pressure in the spectrometer was always below $5 \times 10^{-7}$ Pa. The system was calibrated according to ISO 15472:2001 with an accuracy of ±0.1 eV.

During the sputter depth profile, data acquisition, which was performed using a beam size of 200 μm, with a power of 50 W in a constant-analyzer-energy (CAE) mode with a pass energy of 55 eV (full-width-at-half-maximum (FWHM) of the peak height for Ag $3d_{5/2} = 0.71$ eV), was alternated with $Ar^+$ ion sputtering (18 s at 3 kV, $3 \times 3$ $mm^2$). The sputtering rate was measured on a $Si/SiO_2$ reference sample under the same experimental conditions and found to be 11.6 ± 0.1 nm/min (the standard deviation of the sputtering rate was calculated over three profiles acquired on the same sample). The sputtering depth profiles were processed using MultiPak™ software (v8.1, ULVAC-PHI, Chanhassen, MN, USA). After applying an iterated Shirley-Sherwood background subtraction to the spectra, the apparent atomic in-depth concentration was calculated as:

$$X_j = \frac{I_{ij}/S_{ij}}{\sum_j I_{ij}/S_{ij}} \quad (1)$$

where $I_{ij}$ and $S_{ij}$ are the area and the sensitivity factor of the peak $i$ of the element $j$, respectively. The sensitivity factors were calculated from the Scofield photoionization cross-section [32], the angular asymmetry factor [33, 34], the

spectrometer transmission function and the inelastic mean free path (IMFP) corrected for the emission angle, assuming the sample to be homogenous.

The inelastic mean free path, i.e. the mean distance travelled by electrons with a given kinetic energy (KE) between inelastic collisions in a material $M$, corrected for the emission angle ($\Theta$) was calculated as:

$$\Lambda_{i,M} = \left(\frac{A}{\mathrm{KE}^2} + B \cdot \sqrt{\mathrm{KE}}\right) \cdot \cos\theta(\mathrm{nm}) \quad (2)$$

where the values of $A$ and $B$ were 641 and 0.096, respectively. According to [35], these values are valid for inorganic compounds.

## 3 Results

### 3.1 Characterization of Purified b-TPPT and n-TPPT

#### *3.1.1 Microelemental Analysis*

The microelemental analyses of b-TPPT and n-TPPT after purification by liquid chromatography are reported in Table 2 together with the expected weight percentages. The compositions were found to correspond to the molecular formulas $C_{23}H_{25}O_3PS$ and $C_{45}H_{69}O_3PS$ for b-TPPT and n-TPPT, respectively. The results of the microelemental analysis suggest that the average degree of substitution (DS) per molecule of the phenyl rings of purified b-TPPT with t-butyl groups is one, while the average DS of the phenyl rings of purified n-TPPT with nonyl groups is three.

#### *3.1.2 Fourier Transform Infrared Spectroscopy (FT-IR)*

The transmission FT-IR spectra of b-TPPT and n-TPPT after purification by liquid chromatography (Fig. 2) clearly

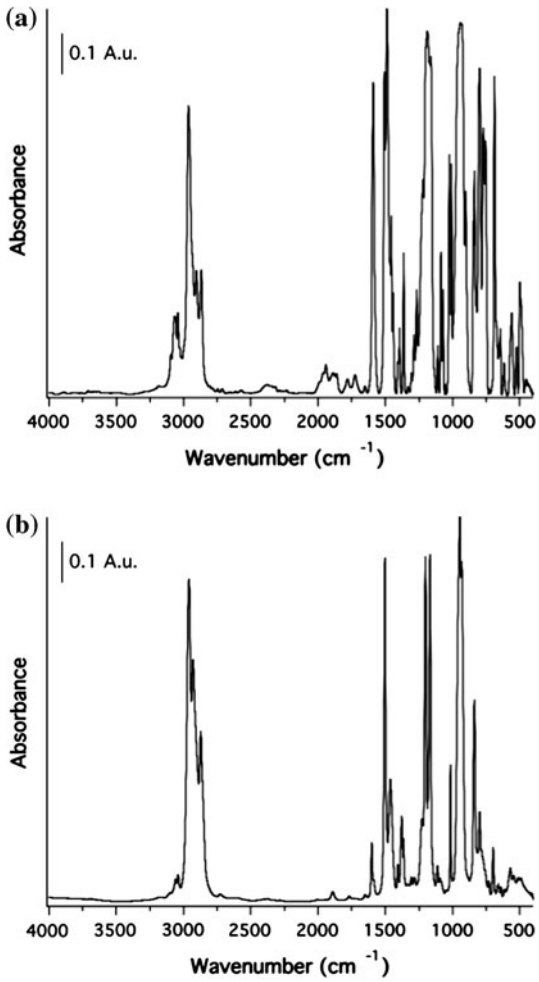


**Fig. 2** Transmission FT-IR spectra of purified alkylated triphenyl phosphorothionates (TPPTs): **a** *t*-butyl triphenyl phosphorothionate (b-TPPT), **b** *p*-nonyl triphenyl phosphorothionate (n-TPPT). Three spectral regions can be distinguished: (i) 3150–2800 $cm^{-1}$: aromatic CH stretching vibrations and alkane $CH_3$, $CH_2$ stretching vibrations; (ii) 2100–1650 $cm^{-1}$: overtone and combination bands due to the aromatic CH out-of-plane deformation vibrations; (iii) 1600–400 $cm^{-1}$ the fingerprint region

**Table 2** Elemental analysis of purified alkylated triphenyl phosphorothionates (*t*-butyl triphenyl phosphorothionate (b-TPPT) and *p*-nonyl triphenyl phosphorothionate (n-TPPT))

| Element | Concentration (wt.%) | | | | | |
|---|---|---|---|---|---|---|
| | b-TPPT | | | | n-TPPT | |
| | Measured | Expected | | | Measured | Expected |
| | | Tri-substituted | Bi-substituted | Mono-substituted | | |
| C | $66.4_6 \pm 0.1_6$ | 70.56 | 68.70 | 66.31 | $74.9_7 \pm 0.1_5$ | 74.96 |
| H | $6.05 \pm 0.01$ | 7.70 | 6.87 | 5.82 | $9.7_4 \pm 0.2$ | 9.65 |
| O | $11.9_7 \pm 0.1_3$ | 9.40 | 10.56 | 12.05 | $6.7_0 \pm 0.1_4$ | 6.66 |
| P | $7.6_8 \pm 0.1_2$ | 6.07 | 6.81 | 7.77 | $4.27 \pm 0.01$ | 4.30 |
| S | $7.84 \pm 0.09$ | 6.28 | 7.05 | 8.05 | $4.4_7 \pm 0.1$ | 4.45 |
| Molecular formula | $C_{23}H_{25}O_3PS$ | $C_{30}H_{39}O_3PS$ | $C_{26}H_{31}O_3PS$ | $C_{22}H_{23}O_3PS$ | $C_{45}H_{69}O_3PS$ | $C_{45}H_{69}O_3PS$ |

**Table 3** IR frequencies ($cm^{-1}$) and functional groups for the transmission FT-IR spectra of purified alkylated triphenyl phosphorothionates (*t*-butyl triphenyl phosphorothionate (b-TPPT) and *p*-nonyl triphenyl phosphorothionate (n-TPPT))

| Frequency ($cm^{-1}$) | | Functional group |
|---|---|---|
| b-TPPT | n-TPPT | |
| 3096 w, 3061, 3043 | 3060, 3041w | $\nu$CH aromatic |
| 2963 s, 2905, 2869 | 2960 vs, 2930, 2872 | $\nu$ Alkane groups |
| 1941,1887, 1862, 1780, 1724, 1652 | 1890, 1768, 1651 | Overtone and combination bands due to $\gamma$CH aromatic |
| 1591, 1509, 1489 vs | 1602, 1504 vs | $\nu$Ph |
| 1456, 1442 | 1465 m | $\delta_{as}CH_3$ (overlapped with $\delta CH_2$ in the case of n-TPPT) |
| 1395, 1364 | 1408 vw, 1379 | $\delta_s CH_3$ |
| 1331, 1307, 1288, 1268, 1220 | 1308, 1284, 1227 | $\delta$CH aromatic |
| 1188 vs, 1161 | 1203, 1169 vs | $\nu$C–O–(P) |
| 1110, 1087, 1070, 1054, 1024, 1016 | 1113, 1094, 1016 | $\delta$CH aromatic |
| 1008 | | $\nu$Ph |
| 943 b,vs | 946, 934 vs | $\nu$P–O–(C) |
| 902, 846 | | $\gamma$CH aromatic |
| 837 m | 838 m | $\nu$C–C |
| 798 s | 799 w | P=S (I) |
| 771 m | | $\nu_s$P–O–(C) |
| 754 | 699 w | $\gamma$CH aromatic |
| 688 m | 659 vw | P=S (II) |
| 655, 644, 616 | | $\delta$CH aromatic |
| 559 | 570 | $\delta$P–O–Ar |
| 524, 498 | 546 | $\gamma$CH aromatic |

$\nu$ stretching, $\gamma$ out-of-plane deformation vibration, $\delta$ in-plane deformation vibration

revealed the characteristic absorption bands of the b-TPPT and n-TPPT molecules. The IR peaks and the assigned functional groups are listed in Table 3. Three spectral regions could be distinguished:

(i) the region at high wavenumbers (3150–2800 $cm^{-1}$)—aromatic CH stretching vibrations and alkane $CH_3$, $CH_2$ stretching vibrations;
(ii) the region between 2100 and 1650 $cm^{-1}$—overtone and combination bands due to the aromatic CH out-of-plane deformation vibrations; and
(iii) the fingerprint region (1600–400 $cm^{-1}$).

All the reported vibration frequencies are in agreement with the literature [30, 36–42].

### *3.1.3 Nuclear Magnetic Resonance (NMR) Spectroscopy*

The NMR spectra (1-H, 13-C and 31-P) of b-TPPT and n-TPPT after purification by liquid chromatography are shown in Fig. 3.

Both the 1-H and 13-C NMR spectra of b-TPPT showed the characteristic signals of benzene in TPPT (not substituted with any alkyl chain) [21, 43, 44]: in the 1-H spectrum two doublets were found at 7.40 and 7.28 ppm, whereas in the 13-C spectrum four signals were detected at 150.9 (A), 129.9 (C), 125.7 (D) and 121.3 (B) ppm. The partial substitution of the phenyl rings in TPPT with a *t*-butyl group resulted in the presence, in the 1-H spectrum, of a doublet at 7.19 ppm, assigned to protons in substituted benzene [43], and of a singlet at 1.35 ppm, which is characteristic of methyl protons in *t*-butyl [45]. In the 13-C spectrum, two additional peaks were found at 126.7 (D′) and 120.6 (B′) ppm, which were assigned to substituted benzene with a *t*-butyl group in para position [43–45]. Three signals were also detected between 30 and 35 ppm and corresponded to the methyl carbon atoms in *t*-butyl [43, 44]. The 31-P NMR spectrum showed two multiplets at 54.4 and 51.4 ppm, whose integrated intensity ratio was 100:27. The first multiplet can be assigned to unsubstituted TPPT, the second one to mono-substituted b-TPPT [46–48].

Both the 1-H and 13-C NMR spectra of n-TPPT showed the characteristic signals of para-substituted benzene [43, 45]: in the 1-H spectrum two peaks were found at 7.29 and 7.15 ppm, whereas in the 13-C spectrum three signals were detected at 148.4 (A), 127.8 (C) and 120.5 (B) ppm. The intense peaks detected between 0.2 and 2.0 ppm in the 1-H spectrum corresponded to the methyl and methylene protons in the nonyl chain [43, 45]. The integrated intensity ratio of the peaks assigned to the para-substituted benzene and of those assigned to the nonyl chain was found to be 21:100, in agreement with the expected value. In the 13-C

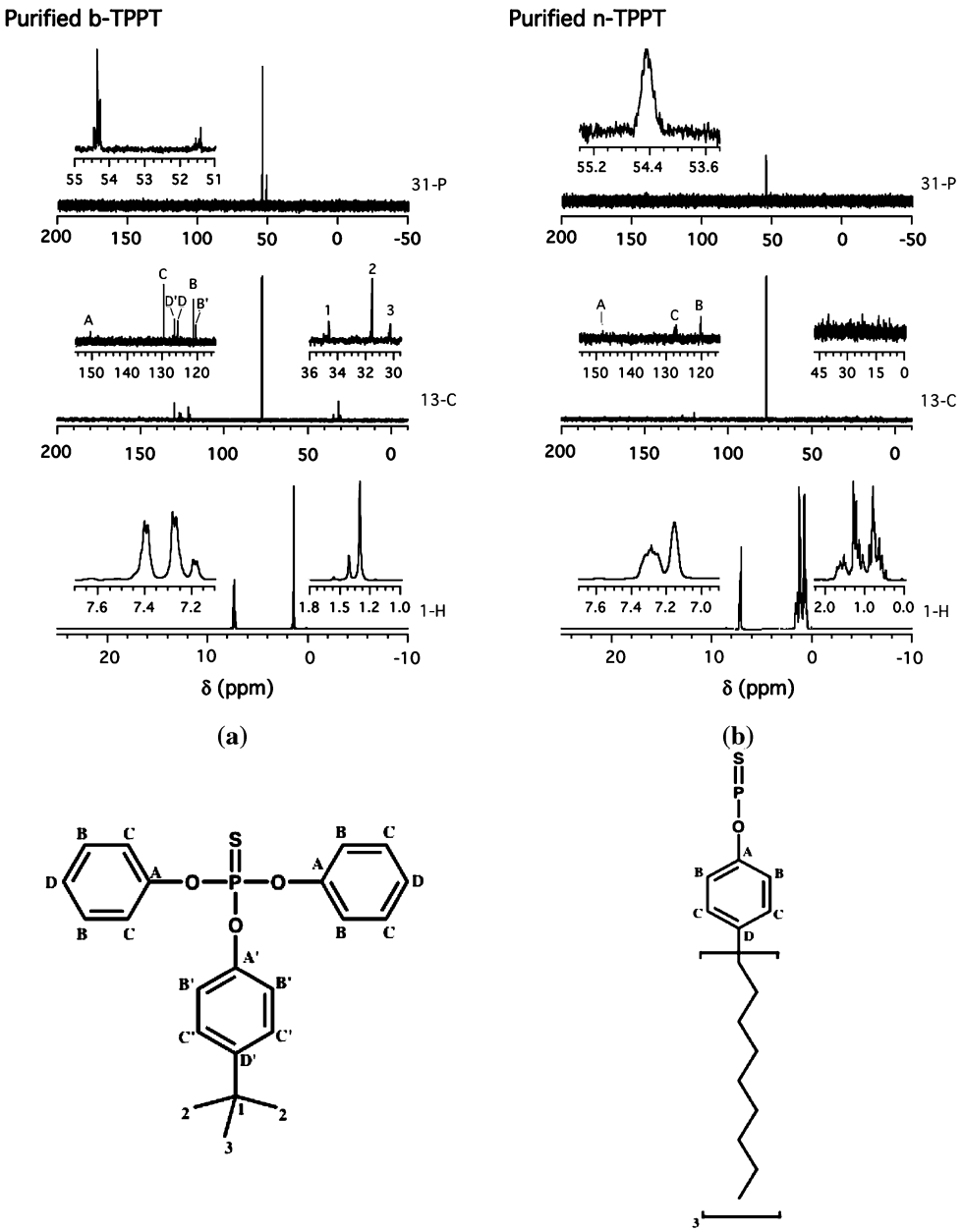


**Fig. 3** NMR spectra (1-H, 13-C and 31-P) of purified alkylated triphenyl phosphorothionates (TPPTs): **a** *t*-butyl triphenyl phosphorotionate (b-TPPT), **b** *p*-nonyl triphenyl phosphorothionate (n-TPPT)

spectrum, the characteristic signals of the nonyl chains between 0 and 45 ppm were very weak [43]. As for the 31-P NMR spectrum, a singlet was detected at 54.4 ppm, in agreement with the literature [46–48].

## 3.2 Heating Experiments

During the heating experiments at 423 K, the oil solutions slowly changed colour, turning yellow-brown after 13–24 h and dark brown after 72–168 h. At 473 K, the color change was faster: they turned yellow after 3 h and dark brown after 24 h.

After the experiments, the solutions were vacuum filtered in order to remove any precipitates formed and the added 100Cr6 steel filings, $Fe_{part}$ and $FeOx_{part}$. No oil-insoluble compounds were ever separated out on the filters.

### *3.2.1 Fourier-Transform Infrared Spectroscopy (FT-IR)*

*3.2.1.1 Heating at 423 K* The transmission FT-IR spectra of a 0.068 mol $dm^{-3}$ solution of b-TPPT in PAO and of a 0.043 mol $dm^{-3}$ solution of n-TPPT in PAO heated at 423 K for 3–168 h are reported in Fig. 4.

The spectra of the unheated solutions (0 h) showed the characteristic peaks of b-TPPT and n-TPPT (Table 3) and PAO (1466 $cm^{-1}$ $\delta_{as}CH_3$ and $\delta CH_2$, 1378 $cm^{-1}$ $\delta_s CH_3$, 890 $cm^{-1}$ $\rho CH_3$, 722 $cm^{-1}$ $\rho CH_2$) [30, 38, 49] molecules.

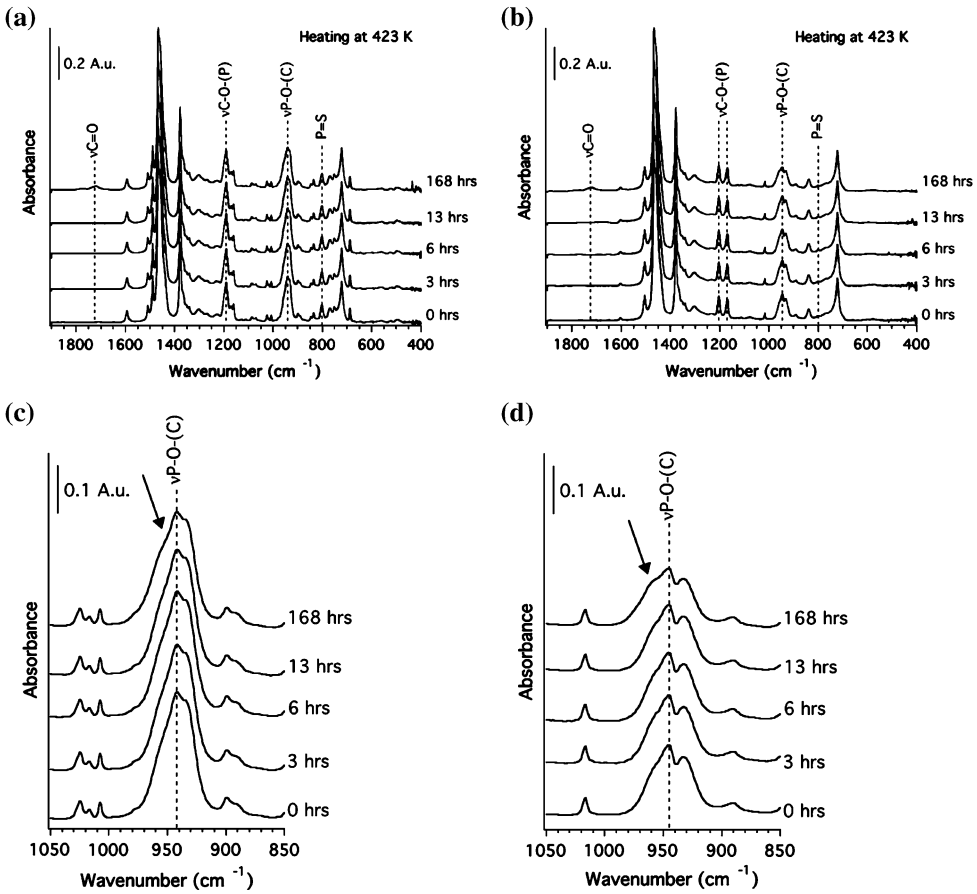


**Fig. 4** Transmission FT-IR spectra of a 0.068 mol $dm^{-3}$ solution of b-TPPT in PAO (**a**)/(**c**) and of a 0.043 mol $dm^{-3}$ solution of n-TPPT in PAO (**b**)/(**d**) heated at 423 K for different times

The C–O–(P) stretching (1190 $cm^{-1}$) and the P=S (I) (802 $cm^{-1}$) vibration bands of b-TPPT in PAO shifted towards higher wavenumbers with respect to the transmission spectrum of purified b-TPPT (Table 3). In the case of the solution of n-TPPT in PAO, no shift of the characteristic bands of the n-TPPT molecule was observed when compared to the transmission FT-IR spectrum of the purified compound (Table 3).

Upon heating at 423 K, no changes in peak position were detected up to 168 h for both the solution of b-TPPT and n-TPPT in PAO. A slight decrease in absorbance of the characteristic vibration bands of b-TPPT (*ν*Ph at 1591 and 1489 $cm^{-1}$, *ν*C–O–(P) at 1190 $cm^{-1}$, *ν*P–O–(C) at 943 $cm^{-1}$ and P=S at 802 $cm^{-1}$) and n-TPPT (*ν*Ph at 1602 and 1504 $cm^{-1}$, *ν*C–O–(P) at 1203 $cm^{-1}$, *ν*P–O–(C) at 946 $cm^{-1}$ and P=S at 799 $cm^{-1}$) was observed after 168 h. A shoulder on the high-wavenumber side of the band assigned to the P–O–(C) stretching vibration was also detected after 168 h for both the solution of b-TPPT (arrow in Fig. 4c) and n-TPPT (arrow in Fig. 4d) in PAO.

In the 1850–1550 $cm^{-1}$ region, where the C=O stretching vibration is found [30, 49], a broad but weak band with maximum at 1720 or 1722 $cm^{-1}$ was detected after 168 h for the solution of b-TPPT or n-TPPT in PAO, respectively. This band exhibited a small peak at higher wavenumbers (at 1771 $cm^{-1}$ or 1769 $cm^{-1}$ for b-TPPT or n-TPPT, respectively).

A slight increase of the baseline in the region between 1300 and 850 $cm^{-1}$, where the C–O stretching vibration is found [30, 49], was also observed after 168 h.

*3.2.1.2 Heating at 473 K* The transmission FT-IR spectra of a 0.068 mol $dm^{-3}$ solution of b-TPPT in PAO and of a 0.043 mol $dm^{-3}$ solution of n-TPPT in PAO heated at 473 K are reported in Fig. 5. The duration of the heating was varied between 3 and 72 h.

A progressive decrease in absorbance of the characteristic vibration bands of b-TPPT (*ν*Ph at 1591 and 1489 $cm^{-1}$, *ν*C–O–(P) at 1190 $cm^{-1}$, *ν*P–O–(C) at 943 $cm^{-1}$ and P=S at 802 $cm^{-1}$) and n-TPPT (*ν*Ph at 1602 and 1504 $cm^{-1}$, *ν*C–O–(P) at 1203 $cm^{-1}$, *ν*P–O–(C) at 946 $cm^{-1}$ and P=S at 799 $cm^{-1}$) was detected upon heating at 473 K. In comparison to the solution heated without any filing/particle, the presence of steel filings or $Fe_{part}$ or $FeOx_{part}$ in the oil solution during the heating experiments turned out to induce a slower decrease in absorbance of the characteristic vibration bands of b-TPPT and n-TPPT.

A shoulder on the high-wavenumber side of the band assigned to the P–O–(C) stretching vibration was detected after 13 h for both the solution of b-TPPT and n-TPPT in

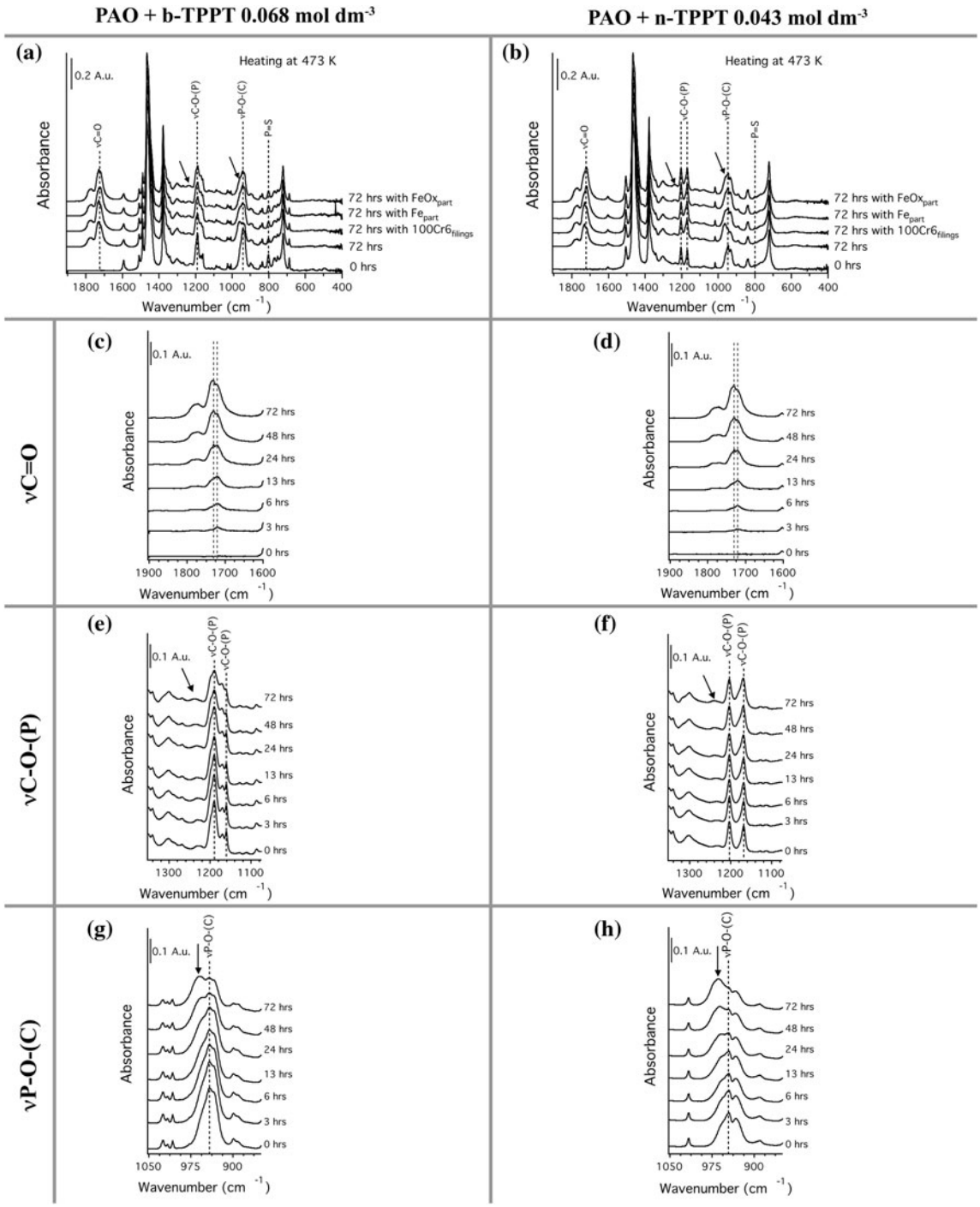


**Fig. 5** Transmission FT-IR spectra of a 0.068 mol $dm^{-3}$ solution of b-TPPT in, PAO (**a**) and of a 0.043 mol $dm^{-3}$ solution of n-TPPT in PAO (**b**) heated at 473 K without any iron particle/steel filings, with 100Cr6 steel filings, metallic iron and iron oxide particles for 72 h. The detailed *ν*C=O, *ν*C–O–(P) and *ν*P–O–(C) regions are reported in **c**–**h** in the case of oil solutions heated at 473 K without any iron particle/steel filings for different times

PAO and found to increase in intensity with the heating time. In the case of the solution of b-TPPT, a well-defined peak at 959 $cm^{-1}$ was detected after 72 h (arrow in Fig. 5a, g). As for the solution of n-TPPT, the shoulder at 959 $cm^{-1}$ turned into a well-defined peak after 24 h. Increasing the heating time induced an increase in intensity of this band and a shift towards higher wavenumbers (961 $cm^{-1}$ after 48 h and 963 $cm^{-1}$ after 72 h) (arrow in Fig. 5b, h). In the case of the solutions (either with b-TPPT or with n-TPPT) heated with filings/particles, the shoulder

on the *v*P–O–(C) band was less intense and no well-defined peak was ever detected (see Fig. 5a, b).

Upon increasing the heating time at 473 K, a broad but weak band at 1241 $cm^{-1}$ was detected for both the solution of b-TPPT and n-TPPT in PAO (arrow in Fig. 5a, b, e, f). The intensity of this new band was not influenced by the presence of steel filings/iron particles ($Fe_{part}$ or $FeOx_{part}$) in the case of the solution containing b-TPPT. As for the oil solution with n-TPPT, a slightly more intense band was detected when the heating experiments were performed in the presence of 100Cr6 steel filings.

A progressive change of the shape of the band assigned to the C–O–(P) stretching vibration was also observed for the solution of b-TPPT heated at 473 K, when compared to the spectrum of the unheated solution (see Fig. 5e). In the case of the n-TPPT solution heated at 473 K, a shoulder at higher wavenumbers characterized the *v*C–O–(P) absorption band at 1169 $cm^{-1}$ (see Fig. 5f). These changes could be due to the superposition of the C–O stretching vibration band at ca. 1175 $cm^{-1}$ as reported in [50].

In the 1850–1550 $cm^{-1}$ region, where the C=O stretching vibration is found [30, 49], a broad band with maximum at 1721 $cm^{-1}$ was detected in the case of the solution of b-TPPT heated with and without 100Cr6 steel filings and found to shift towards higher wavenumbers (1730 $cm^{-1}$) after 24 h. No shift of the absorption band in the 1850–1550 $cm^{-1}$ region, which had a maximum at 1721 $cm^{-1}$, was detected when the heating experiments were carried out in the presence of $Fe_{part}$ or $FeOx_{part}$.

As for the solution of n-TPPT, the broad band at 1721 $cm^{-1}$ (with a small peak at 1770 $cm^{-1}$), which appeared in the transmission FT-IR spectra upon heating at 473 K for 3 h, did not undergo any shift when the heating experiments were performed in the presence of $Fe_{part}$ or $FeOx_{part}$. For the solutions heated without any filing/particle and with 100Cr6 steel filings, a shift towards higher wavenumbers, i.e. 1730 $cm^{-1}$, was found after 24 and 48 h, respectively.

*3.2.1.3 Oxidation of the Base Oil* In order to investigate the influence of alkylated TPPTs on the oxidation of the base oil, the area of the C=O stretching vibration band, after linear baseline subtraction, was plotted as a function of the heating time at 423 and 473 K (Fig. 6). For comparison purposes, control heating experiments on pure base oil (PAO) have been performed at the same temperatures investigated in this work, i.e. 423 and 473 K.

Compared to pure PAO, the presence of b-TPPT and n-TPPT in the solutions strongly reduced the oxidation of the base oil at 423 K (Fig. 6a). The TPPT molecule substituted with nonyl chains was found to reduce the area of the carbonyl peak to a slightly higher extent than the molecule with a *t*-butyl chain bound to the phenyl ring (inset of Fig. 6a).

At 473 K, both b-TPPT and n-TPPT did not reduce the area of the carbonyl peak as effectively as at 423 K. Moreover, the presence of either 100Cr6 steel filings, or $Fe_{part}$ or $FeOx_{part}$ in the oil solution during the heating experiments was found to slightly increase the oxidation of the base oil, when compared to the solutions heated without any filing/particles (Fig. 6b, c).

*3.2.1.4 Degradation Index (DI)* In order to investigate the degradation kinetics, the degradation index (DI) has been defined as:

$$\mathrm{DI} = \frac{A_{t,i}}{A_{0,i}} \cdot 100 \tag{3}$$

where $A_{t,i}$ is the absorbance of the *i*-th vibration at *t* heating hours, while $A_{0,i}$ is the absorbance of the *i*-th vibration for the unheated solution [21].

Figures 7 and 8 report the DI of three characteristic vibrations of b-TPPT ($\nu Ph_{1591cm^{-1}}$, *v*P–O–(C), P=S (I)) and four characteristic vibrations of n-TPPT ($\nu Ph_{1602cm^{-1}}$, $\nu C-O-(P)_{1203cm^{-1}}$, *v*P–O–(C), P=S (I)) for a 0.068 mol $dm^{-3}$ solution of b-TPPT in PAO and a 0.043 mol $dm^{-3}$ solution of n-TPPT in PAO as a function of the heating time at 423 and 473 K.

The DI of the characteristic *v*C–O–(P) vibration of the b-TPPT molecule is not shown in Figs. 7 and 8 since the superposition of the C–O stretching vibration appearing in the transmission FT-IR spectra as a result of the oxidation of the base oil resulted in DI values not representative of the decrease in absorbance of the *v*C–O–(P) band, as already noted in [21]. In the case of n-TPPT, since the C–O stretching vibration of the oxidation products of the base oil was found to be superimposed on the *v*C–O–(P) band at 1169 $cm^{-1}$, the DI of *v*C–O–(P) band at 1203 $cm^{-1}$ has been calculated and shown in Figs. 7 and 8.

At 423 K, all three absorption bands of b-TPPT showed similar values of the DI, which monotonically decreased with the heating time (logarithmic scale on the DI axis). In the case of the solution with n-TPPT, the DI of the four characteristic vibrations of this molecule decreased in the following order: $\nu Ph_{1602cm^{-1}} \approx \nu C-O-(P)_{1203cm^{-1}} >$ *v*P–O–(C) > P=S (I). Comparing the DI of the P=S (I) absorption band for the two different additives, the lowest values were obtained in the case of the solution containing n-TPPT.

An increase in the degradation rate was observed for all absorption bands of b-TPPT and n-TPPT upon heating at 473 K.

In the case of the solution containing b-TPPT, all three bands showed a monotonic decrease of the DI (logarithmic

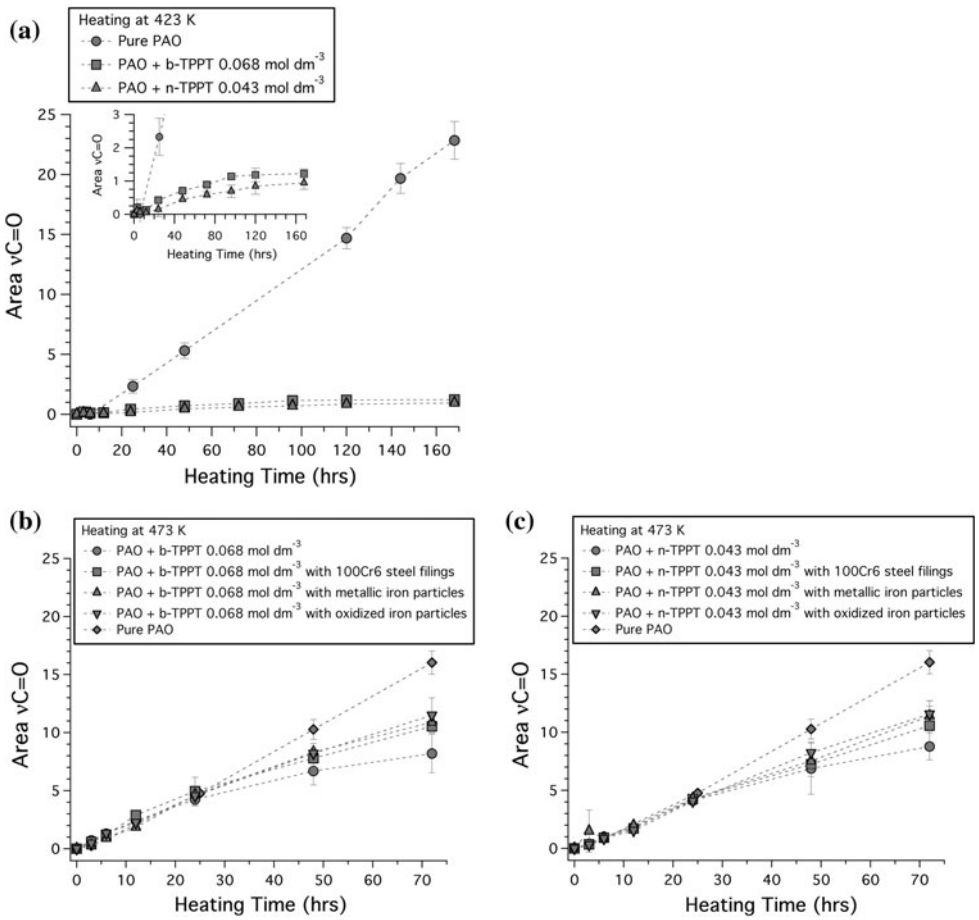


**Fig. 6** Area of the C=O stretching vibration band as a function of the heating time at: **a** 423 K for a 0.068 mol $dm^{-3}$ solution of b-TPPT in PAO and for a 0.043 mol $dm^{-3}$ solution of n-TPPT in PAO; **b** 473 K for a 0.068 mol $dm^{-3}$ solution of b-TPPT in PAO; **c** 473 K for a 0.043 mol $dm^{-3}$ solution of n-TPPT in PAO. The values of the area of the C=O stretching vibration band for pure PAO heated at the same temperatures are included for comparison

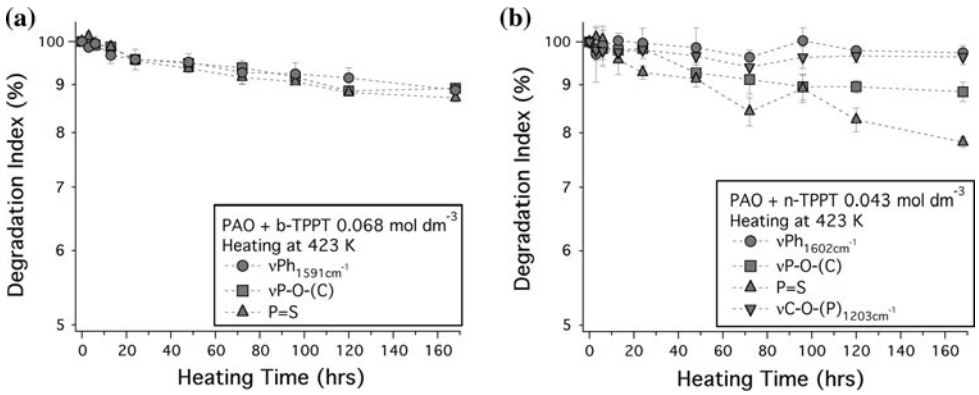


**Fig. 7** Degradation Index (DI) versus heating time at 423 K for the characteristic vibrations of b-TPPT (**a**) and n-TPPT (**b**) in PAO

scale on the DI axis) independently of the presence of 100Cr6 steel filings, $Fe_{part}$ and $FeOx_{part}$. The DI values of the three vibrations were comparable for the solutions heated in the presence of $Fe_{part}$, whereas in the case of the experiments carried out with steel filings or $FeOx_{part}$, the P=S (I) band had a *DI* slightly lower than the other two peaks considered above. As for the solution heated without any filings/particles, the DI values of all three absorption bands were lower than in the case of the solutions heated with filings/particles and decreased in the following order: $\nu Ph_{1591cm^{-1}} > \nu P–O–(C) > P=S$ (I).

In the case of the solution with n-TPPT heated at 473 K without any filings/particles, the four characteristic absorption bands of n-TPPT showed a monotonic decrease of the DI (logarithmic scale on the DI axis) with the heating time. Moreover, the DI values decreased in the following

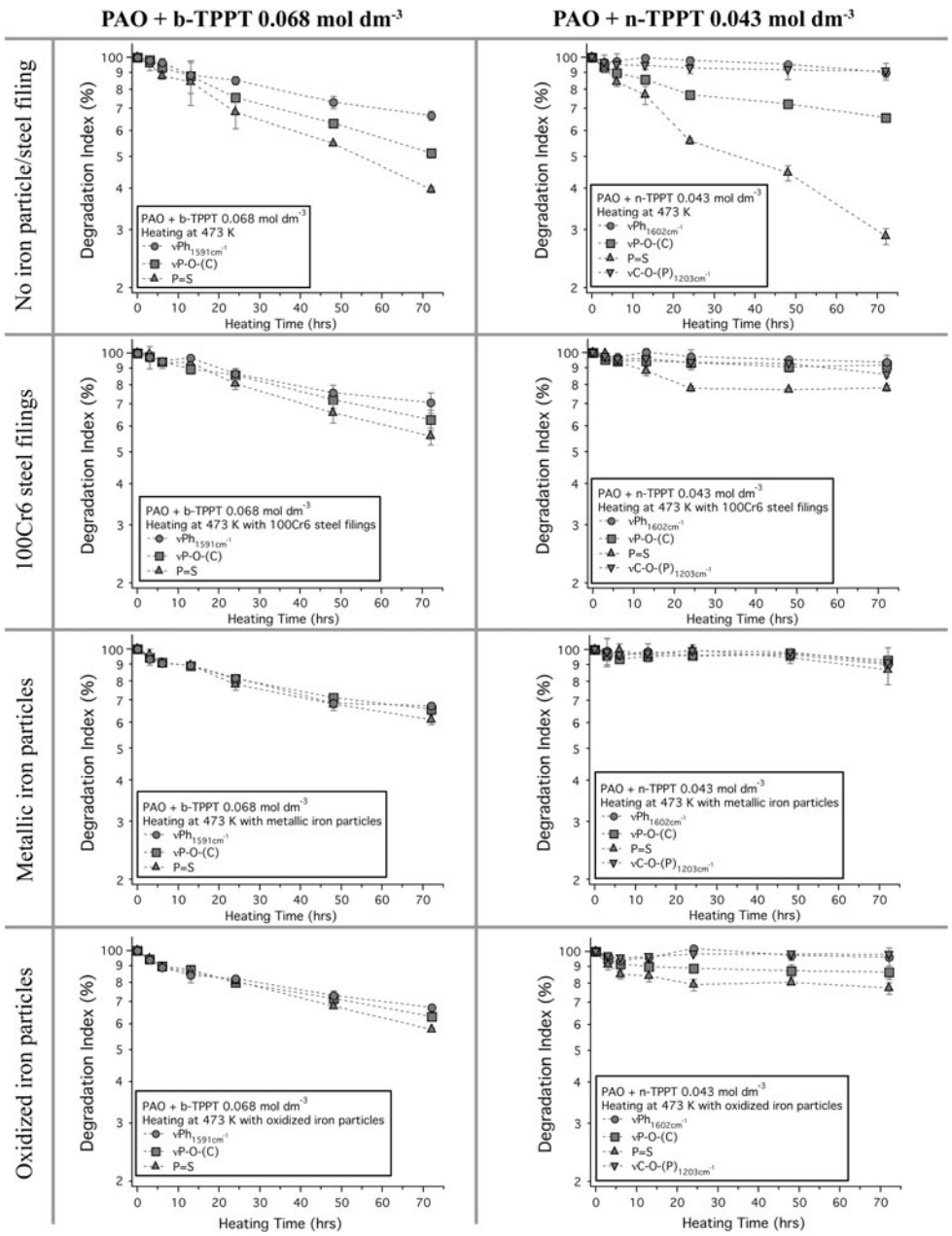


**Fig. 8** Degradation Index (DI) versus heating time at 473 K for the characteristic vibrations of b-TPPT and n-TPPT in PAO

order: $\nu Ph_{1602cm^{-1}} \approx \nu C-O-(P)_{1203cm^{-1}} > \nu P–O–(C) >$ P=S (I). When the heating experiments were performed in the presence of steel filings or iron particles ($Fe_{part}$ or $FeOx_{part}$), higher values of the DI were obtained. In contrast to the solution heated with $Fe_{part}$, for which the DI of the characteristic vibrations of n-TPPT had comparable

values, in the case of the experiments performed with steel filings or $FeOx_{part}$ the P=S (I) band had slightly lower DI values than the other vibrations considered above.

### 3.2.2 Nuclear Magnetic Resonance (NMR) Spectroscopy

The NMR spectra (1-H, 13-C and 31-P) of 0.068 mol $dm^{-3}$ solutions of b-TPPT and of 0.043 mol $dm^{-3}$ solutions of n-TPPT in PAO heated at 423 and 473 K are shown in Fig. 9 together with the spectra of the unheated solutions. In the 1-H and 13-C spectra, since the signals assigned to the *t*-butyl and nonyl chains bound to the phenyl ring of, respectively, the b-TPPT and n-TPPT molecules are superposed on those of PAO (i.e. between 0 and 2 ppm in the 1-H spectrum and between 10 and 45 ppm in the 13-C spectrum), only the regions where the benzene peaks are detected, are shown.

In the spectra of the unheated solutions, the characteristic peaks of b-TPPT and n-TPPT were found.

In the 1-H and 13-C NMR spectra of solutions of b-TPPT and n-TPPT in PAO heated at 423 and 473 K (with and without filings/particles), no new peaks appeared in the region where the characteristic signals of benzene are found. New but weak peaks appeared in the 6–2 ppm region (not shown) of the 1-H spectra of the solutions heated at 473 K with and without steel filings and iron particles ($Fe_{part}$ or $FeOx_{part}$) and can be assigned to hydrogen of a methyl or methylene group bound to a carbonyl or ester group [45]. No signals that can be assigned to these species, can be found in the 13-C spectra due to the small magnetic moment and low natural abundance of carbon-13 [43, 44].

In the 31-P spectrum of the unheated solution of b-TPPT (0 h), two multiplets at 54.5 and 51.5 ppm were detected, whose integrated intensity ratio was 100:29 ± 2. Upon heating at 423 K for 168 h, new but weak peaks were found at −15.7, −16.0, −16.3, −16.9 and −17.2 ppm (integrated intensity ratio of the multiplets at 54.5, 51.5 and of the signals between −15.5 and −17.5 ppm: $I_{54.5\ ppm}$:$I_{51.5\ ppm}$:$I_{-15.5/-17.5\ ppm}$ = 100:32 ± 1:6 ± 1). Upon increasing the temperature to 473 K, the peaks appearing at higher field than the characteristic signals of b-TPPT increased in intensity: the integrated intensity ratio $I_{54.5\ ppm}$:$I_{51.5\ ppm}$:

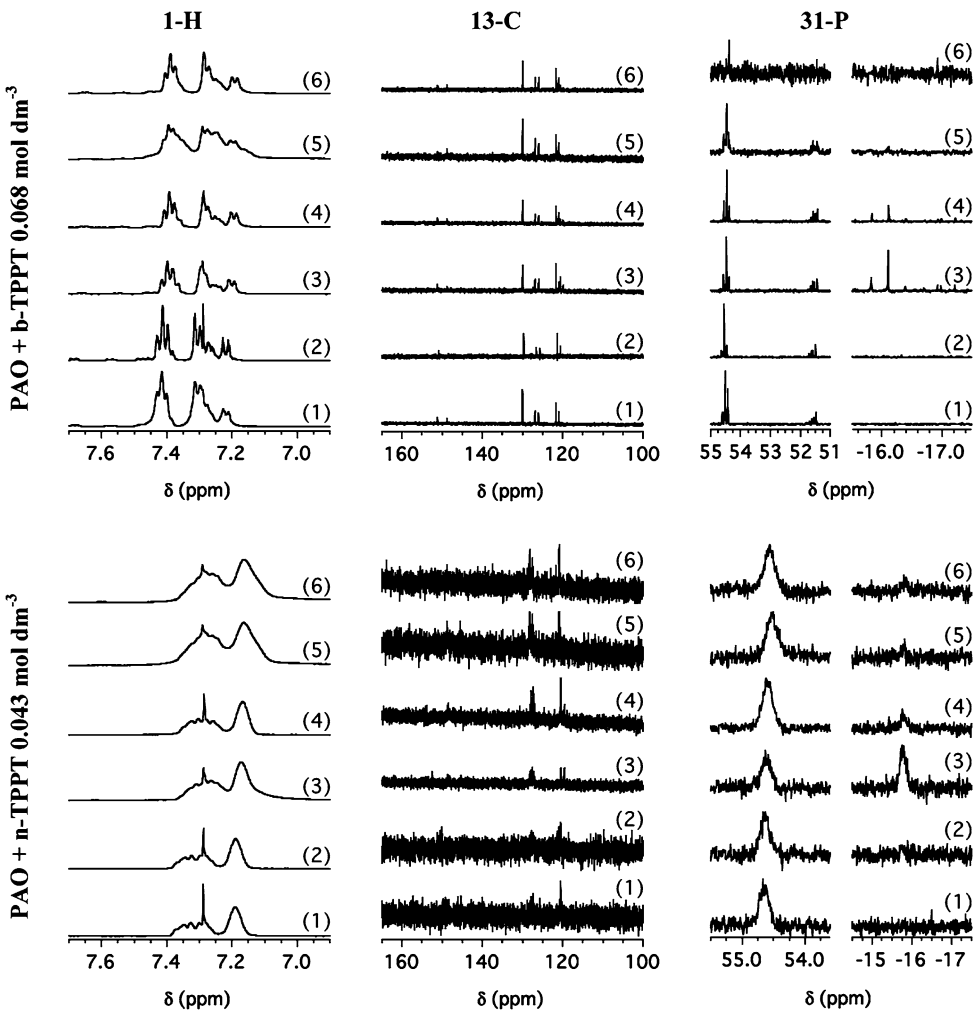


**Fig. 9** NMR spectra (1-H, 13-C and 31-P) of 0.068 mol $dm^{-3}$ solutions of b-TPPT and of 0.043 mol $dm^{-3}$ solutions of n-TPPT in PAO: (*1*) unheated; (*2*) heated at 423 K for 168 h without any iron particle/steel filing; (*3*) heated at 473 K for 72 h without any iron particle/steel filing; (*4*) heated at 473 K for 72 h with 100Cr6 steel filings; (*5*) heated at 473 K for 72 h with metallic iron particles; and (*6*) heated at 473 K for 72 h with iron oxide particles

$I_{-15.5\ ppm}$ was found to be 100:39 ± 2:68 ± 4. When the heating experiments were performed in the presence of steel filings or iron particles ($Fe_{part}$ or $FeOx_{part}$), the peaks between −15.5 and −17.5 ppm were less intense. In the case of the solution heated with 100Cr6 steel filings, the integrated intensity ratio $I_{54.5\ ppm}$:$I_{51.5\ ppm}$:$I_{-15.5\ ppm}$ was 100:39 ± 2:29 ± 3. As for the solution heated in the presence of $Fe_{part}$, a weak signal at −16.1 ppm was detected ($I_{54.5\ ppm}$:$I_{51.5\ ppm}$:$I_{-16.1\ ppm}$ was 100:33 ± 1:8 ± 2), while no new peaks appeared in the high-field region of the 31-P spectrum of the solution heated with $FeOx_{part}$.

In the case of the unheated solution of n-TPPT in PAO, a singlet at 54.6 ppm was detected in the 31-P spectrum. No new peaks were found in the spectrum of the solution heated at 423 K for 168 h. Upon heating at 473 K for 72 h with and without steel filings or iron particles ($Fe_{part}$ or $FeOx_{part}$), a new signal was detected at −15.8 ppm. The intensity of this peak was lower when the heating experiments were performed in the presence of steel filings or iron particles ($Fe_{part}$ or $FeOx_{part}$): in the case of the solution heated at 473 K without any filing/particle the integrated intensity ratio of the peak at 54.6 and −15.8 ppm ($I_{54.6\ ppm}$:$I_{-15.8\ ppm}$) was 100:128 ± 3 and decreased to 100:26 ± 3 for the solution heated with 100Cr6 steel filings. In the case of the heating experiments carried out with $Fe_{part}$ and $FeOx_{part}$, the ratio was 100:9 ± 1 and 100:11 ± 2, respectively.

### 3.2.3 XPS Sputtering Depth Profile

The depth distribution of the elements present in the reaction layers formed on the 100Cr6 steel filings immersed in the b-TPPT and n-TPPT solutions heated at 473 K for 72 h was determined by XPS sputter depth profiling. The apparent atomic concentration is reported in Fig. 10 as a function of the sputtering time.

On the filings' surfaces only carbon, oxygen, phosphorus and iron were detected (spectra not shown). Upon sputtering, the carbon concentration progressively decreased, indicating the removal of an organic layer. The oxygen profile had a maximum after 3.9 min (corresponding to a sputtering depth of 45.2 ± 0.4 nm relative to a $Si/SiO_2$ reference sample) and 3.0 min (corresponding to a sputtering depth of 34.8 ± 0.3 nm relative to a $Si/SiO_2$ reference sample) for the reaction layer formed in the presence of b-TPPT and n-TPPT, respectively. As for phosphorus, a peak at 134.4 ± 0.1 and 134.3 ± 0.1 eV (referencing the aliphatic carbon to 285.0 eV), values typical for phosphate/polyphosphate compounds [51, 52], was detected before the sputtering (0 min sputtering time) in the high-resolution (HR) spectra of the films generated from b-TPPT and n-TPPT, respectively. The phosphorus concentration increased with the sputtering time, reached a maximum after 3.0 min (corresponding to a sputtering depth of 34.8 ± 0.3 nm relative to a $Si/SiO_2$ reference sample) and 2.4 min (corresponding to a sputtering depth of 27.8 ± 0.2 nm relative to a $Si/SiO_2$ reference sample) for the layers formed from b-TPPT and n-TPPT, respectively, and went to zero after 6.6 min (corresponding to a sputtering depth of 76.6 ± 0.7 nm relative to a $Si/SiO_2$ reference sample) of sputtering. No sulphur was ever detected in either reaction-layer sample during the sputter depth profiling.

## 4 Discussion

### 4.1 Antioxidant Property of Alkylated TPPTs

Lubricating oils are susceptible to thermo-oxidative ageing. The mechanism of hydrocarbon oxidation at high

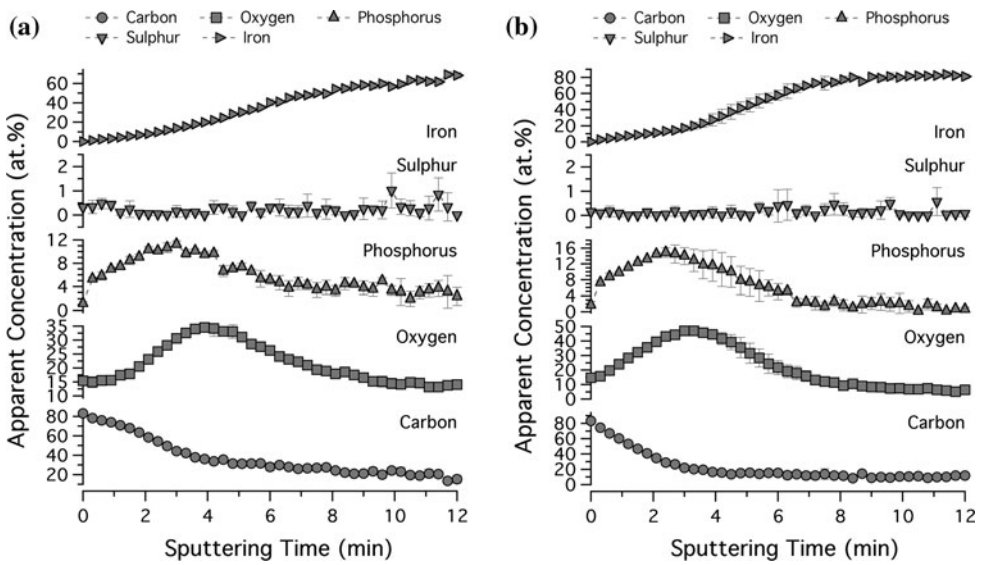


**Fig. 10** X-ray photoelectron spectroscopy (XPS) sputtering depth profile ($Ar^+$ ion sputtering at 3 kV, 3 × 3 $mm^2$) of a 100Cr6 steel filing immersed in a 0.068 mol $dm^{-3}$ solution of b-TPPT in PAO (**a**) and in a 0.043 mol $dm^{-3}$ solution of n-TPPT in PAO (**b**) heated at 473 K for 72 h

temperatures has been thoroughly investigated: it is driven by an autocatalytic process involving a four-step free-radical reaction (initiation of the radical chain reaction, chain propagation, chain branching and termination of the radical chain reaction), which leads to the formation of a complex mixture of oxygenated products, such as hydroperoxides, alkyl peroxides, alcohols, carboxylic acids, peroxy acids, esters, ketones, aldehydes, lactones, etc. [8, 22, 23].

As observed in our previous studies [21, 24], the appearance of a broad absorption band between 1850 and 1550 $cm^{-1}$ and the increase of the baseline in the 1300–850 $cm^{-1}$ region in the FT-IR spectra, as well as the presence of new peaks between 6 and 2 ppm in the 1-H NMR spectra of solutions containing either b-TPPT or n-TPPT heated at 423 and 473 K with and without steel filings or iron particles ($Fe_{part}$ or $FeOx_{part}$), clearly indicate that the base oil (PAO) was getting oxidized during the heating process.

The presence of several overlapping peaks (corresponding to different carbonyl compounds [30, 49, 50, 53]) contributing to the complex envelope at 1850–1550 $cm^{-1}$ in the FT-IR spectra makes it difficult to identify the chemical nature and distribution of the species produced during the oxidation of the base oil. The shift of the peak maximum in the 1850–1550 $cm^{-1}$ region of the FT-IR spectra of the solution of b-TPPT and n-TPPT heated at 473 K with and without 100Cr6 steel filings as the heating time increased, i.e. as the base oil got oxidized, might be due to the different distributions of the oxidation products, as already noted in [21, 24]. Moreover, the shift towards lower wavenumbers of the carbonyl band when the heating experiments were carried out in the presence of $Fe_{part}$ or $FeOx_{part}$, suggests that the oxidation reaction pathway of the base oil is influenced by the presence of iron particles.

The absorption band found in the FT-IR spectra of the solution of b-TPPT and n-TPPT heated at 423 and 473 K at ca. 1771 $cm^{-1}$ can be assigned to five-membered-ring lactones and to small amounts of peroxy esters, while the peak at 1731–1720 $cm^{-1}$ is expected to correspond to ester compounds [30, 49, 50, 53].

In the final stage, i.e. after heating the oil solutions at 423 K for 168 h and at 473 K for 72 h, the characteristic peaks of the b-TPPT and n-TPPT molecules were still detected in the FT-IR spectra. This finding, together with the appearance of the complex carbonyl absorption band between 1850 and 1550 $cm^{-1}$, suggests that both the b-TPPT and n-TPPT molecules are not effective oxidation inhibitors, as opposed to ZnDTPs, which are known to act as both primary (radical trapping) and secondary (peroxide-decomposing) antioxidants [6–9].

In order to gain an insight into the impact of b-TPPT and n-TPPT as well as into the effect of the added 100Cr6 steel filings, $Fe_{part}$ and $FeOx_{part}$ on the oxidation of the base oil, the area of the carbonyl peak appearing between 1850 and 1550 $cm^{-1}$ in the FT-IR spectra was plotted as a function of the heating time. For comparison purposes, control heating experiments on pure PAO have been performed at the same temperatures investigated in this work, i.e. 423 and 473 K.

Compared to pure PAO, the presence of b-TPPT and n-TPPT in the oil solutions effectively reduced the area of the carbonyl peak at 423 K, indicating that the additives have a strong antioxidant effect at this temperature. The comparison of these findings with the results of the FT-IR analysis of solutions of TPPT (without any alkyl chain attached to the phenyl ring) in PAO heated at 423 K, presented in our previous work [21], allows the effect of the substituent in the TPPT molecules on the oxidation of the base oil to be investigated: the longer the alkyl chain bound to the phenyl rings, the larger the reduction of the area of the carbonyl peak at 423 K, i.e. the stronger the antioxidant effect.

At 473 K, neither b-TPPT nor n-TPPT was found to inhibit the oxidation of the base oil as effectively as at 423 K. Compared to TPPT [21], the presence of an alkyl chain (either *t*-butyl or *p*-nonyl) bound to the phenyl rings turned out to reduce the area of the carbonyl peak to a slightly higher extent when the solutions were heated with and without 100Cr6 steel filings, while no significant difference was observed in the case of the experiments carried out with $Fe_{part}$ or $FeOx_{part}$.

The presence of transition metal ions having two valence states is known to lower the activation energy of the decomposition process of the alkyl hydroperoxide molecules formed during the autoxidation of hydrocarbons at high temperatures [8]. This explains the catalytic effect of steel filings and iron particles ($Fe_{part}$ or $FeOx_{part}$) on the oxidation of the base oil observed in the case of the lubricant solutions containing b-TPPT and n-TPPT heated at 473 K. As for the solutions of TPPT heated at 473 K, the oxidation of the base oil was not catalyzed by the presence of steel filings or iron particles ($Fe_{part}$ or $FeOx_{part}$) [24].

### 4.2 Influence of the Alkyl Chain Length and Iron Oxidation State on the Reactivity of Alkylated TPPTs in Oil Solution

As was observed in the case of solutions of TPPT in PAO [21, 24], the transmission FT-IR and NMR spectra showed the presence of the characteristic signals of the b-TPPT and n-TPPT molecules even after heating at 423 K for 168 h and at 473 K for 72 h. During the heating experiments, no oil-insoluble compounds were ever detected. These findings suggest that the alkylated TPPTs are highly thermally stable in oil solution, even in the presence of steel filings or iron particles ($Fe_{part}$ or $FeOx_{part}$). ZnDTP, in contrast, is known to completely react at high temperature (403–503 K) within a few hours to produce a precipitate,

whose composition is similar to that of the films formed on tribological surfaces [6, 10, 54–56].

Although the oil solutions started to change color after 13–24 h at 423 K and after 3 h at 473 K, a shoulder on the high-wavenumber side of the *v*P–O–(C) peak was found only after heating for 168 h at 423 K and for 13 h at 473 K. A broad but weak band was also detected at 1241 $cm^{-1}$ for both the solution of b-TPPT and n-TPPT in PAO heated at 473 K, which can be assigned to the P=O stretching vibration [30]. The presence of this band suggests the exchange of the sulphur atom in the alkylated TPPTs molecules with a phosphoryl oxygen, as reported by Teichmann and Hilgetag [15] and as proposed in our previous studies in the case of solutions of TPPT in PAO heated at 423 and 473 K with and without steel filings or iron particles ($Fe_{part}$ or $FeOx_{part}$) [21, 24]. The presence of an electron withdrawing oxygen bound to the phosphorus atom also explains the appearance of a shoulder at higher wavenumbers in the *v*P–O–(C) peak [42, 57].

These band assignments could be confirmed by the NMR analyses. In the 31-P NMR spectra new peaks were found at higher fields (between −15.5 and −17.5 ppm) compared to the characteristic signals of the starting compounds, i.e. b-TPPT and n-TPPT, and corresponded to alkylated triphenyl phosphates (butylated triphenyl phosphate (b-TPP) and nonylated triphenyl phosphate (n-TPP), respectively) [46, 47]. The presence of the alkyl chain, either *t*-butyl in the case of b-TPP or *p*-nonyl in the case of n-TPP, bound to the phenyl rings is suggested by the 1-H spectra, which did not exhibit the appearance of any new peak in the region where the characteristic signals of benzene are found. In the case of the oil solutions containing b-TPPT, the detection of several peaks between −15.5 and −17.5 ppm in the 31-P NMR spectra could be due to the presence of different isomers of the b-TPP molecule [46].

As was the case for solutions of TPPT in PAO heated at 473 K [24], the signal at higher fields (between −15.5 and −17.5 ppm) in the 31-P NMR spectra decreased in intensity when either 100Cr6 steel filings, or $Fe_{part}$ or $FeOx_{part}$ were added to the oil solutions containing b-TPPT and n-TPPT during the heating experiments. This finding, together with the corresponding decrease in intensity of the shoulder on the high-wavenumber side of the *v*P–O–(C) peak in the FT-IR spectra, suggests that the amount of alkylated triphenyl phosphates present in the lubricant was lower when the heating experiments were carried out in the presence of steel filings or iron particles ($Fe_{part}$ or $FeOx_{part}$). Such a lower concentration of alkylated TPPs in the oil solution can be explained in two possible ways: either these molecules react on the surface of steel filings/iron particles and form a reaction layer, as indicated by the XPS sputter depth profile of the 100Cr6 steel filings immersed for 72 h in oil solutions heated at 473 K, and/or the oxygen present in the oil preferentially takes part in the oxidation reaction of PAO (catalyzed by steel filings and iron particles ($Fe_{part}$ or $FeOx_{part}$)) rather than in that of alkylated TPPTs. The absence of any signal that can be assigned to intermediate species in the thermo-oxidative reaction of alkylated TPPTs, such as phosphites, for example, suggests that the reaction of alkylated TPPs on the filings/particles surface is the main reason for their lower concentration in oil solutions.

In our previous studies, a further insight into the degradation kinetics of TPPT in oil solution was provided by the DI [21, 24]. The scission of the P=S bond as a starting point in the thermal reaction of TPPT was suggested by the DI values of the corresponding absorption band in the FT-IR spectra, which were always lower than the values of the Ph and P–O–(C) stretching vibration peaks. Moreover, the influence of the iron oxidation state on the degradation kinetics of TPPT could also be investigated: even if the reaction pathway turned out not to be affected by the presence of steel filings or iron particles ($Fe_{part}$ or $FeOx_{part}$) in the lubricant solution, i.e. the scission of the thiophosphoryl bond still started the decomposition reaction, the thermal degradation of TPPT was found to be catalyzed by the metallic iron particles.

In the present work, the DI of the characteristic vibration bands of the b-TPPT and n-TPPT molecules was calculated in order to have an insight into the reaction pathway as well as into the influence of temperature, alkyl chain length and iron oxidation state on the degradation kinetics.

As was the case for TPPT, the scission of the P=S bond turned out to be the starting point of the thermo-oxidative reaction of alkylated TPPTs at 423 and 473 K. Only in the case of the b-TPPT solution heated at 423 K, can a definitive statement about the reaction pathway not be made on the basis of the DI, since all the vibration bands considered had comparable DI values. As for the n-TPPT molecule, the superposition of the C–O stretching vibration of the oxidation products of the base oil upon the *v*C–O–(P) band at 1169 $cm^{-1}$ allowed the DI of the *v*C–O–(P) band at 1203 $cm^{-1}$ to be calculated. As a consequence, the reaction step following the P=S bond scission could be identified on the basis of the FT-IR spectra: the cleavage of the P–O bond seems to preferentially occur over the breakage of the C–O bond.

The comparison of the DI of the P=S bond for solutions of b-TPPT and n-TPPT in PAO heated at 473 K with and without steel filings or iron particles ($Fe_{part}$ or $FeOx_{part}$) also allowed the influence of the iron oxidation state on the degradation kinetics of alkylated TPPTs to be investigated. Compared to the solution heated without any filings/particles, the presence of either 100Cr6 steel filings, or $Fe_{part}$ or $FeOx_{part}$ in the oil solution containing either b-TPPT or n-TPPT during the heating process resulted in slightly higher DI values, indicating that the kinetics of the

thermo-oxidative reaction is slower. Moreover, while in the case of b-TPPT no significant difference in the DI of the P=S band was observed between the solutions heated with steel filings and iron particles ($Fe_{part}$ or $FeOx_{part}$), in the case of the solutions containing n-TPPT the presence of $Fe_{part}$ during the heating process resulted in DI values slightly higher than those calculated for the lubricants heated in the presence of 100Cr6 steel filings or $FeOx_{part}$. These findings can be explained with the catalytic effect of steel filings and iron particles ($Fe_{part}$ or $FeOx_{part}$) on the oxidation of the base oil, as indicated by the FT-IR results. As a consequence of the preferential reaction of the oxygen present in the oil solution with the base oil, the kinetics of the thermo-oxidative reaction of alkylated TPPTs is slower.

A comparison with the data presented in our previous work can provide an insight into the effect of the length of the alkyl chain bound to the phenyl rings on the degradation reaction [21, 24]. At 423 K, the TPPT molecule (not substituted with any alkyl chain) turned out to be more reactive than alkylated TPPTs (with n-TPPT being more reactive than b-TPPT). At 473 K, the reactivity of TPPT and n-TPPT was found to be similar but higher than that of b-TPPT. In the case of the experiments carried out in the presence of steel filings or iron particles ($Fe_{part}$ or $FeOx_{part}$), the reactivity of the TPPTs was demonstrated to decrease with alkyl chain length.

Two effects might be taken into consideration for explaining this difference in the reactivity of TPPTs: electronic and solubility effects. As for the former, the presence of electron-releasing (ER) groups bound to the phenyl rings of arylphosphorothionates has been reported to increase the P=S bond length and the charge on the phosphorus atom [58]. This would make the phosphorus atom itself more open to nucleophilic attack, increasing, as a consequence, the reactivity of the molecule. Therefore, the electronic effect induced by the substitution of TPPT with alkyl chains does not explain the decrease in reactivity observed in the present paper.

On the other hand, the presence of an alkyl chain attached to the aromatic ring enhances the solubility of the molecule in lubricant oil, which would result in a lower amount of adsorbed additive at the steel (or iron)/oil interface. The different solubility in lubricant oil of the triphenyl phosphorothionate molecules employed in the present work and in our previous ones [21, 24] can, then, explain the difference in the reactivity of these compounds in lubricant oil at high temperature.

### 4.3 Role of the Alkyl Chain in the Surface Chemistry of Alkylated TPPTs

A comparison of the results presented in this work with those outlined in our previous study [24] also allows the role of the alkyl chain in the surface chemistry of alkylated TPPTs to be clarified. While in the case of TPPT (without any alkyl chain bound to the phenyl rings) the XPS sputter depth profile of 100Cr6 steel filings immersed for 72 h in oil solution heated at 473 K showed the presence of sulphur starting from a sputtering depth of $3.5 \pm 0.1$ nm (relative to a $Si/SiO_2$ reference sample) [24], the reaction layers formed from alkylated TPPTs (i.e. b-TPPT and n-TPPT) under the same experimental conditions did not contain any sulphur. This finding clearly suggests that the reaction mechanism strongly depends on the architecture of the molecule even within the same class of additives. In the following section a reaction mechanism for alkylated TPPTs will be proposed.

The fact that the reaction layers analysed in the present work differ from those investigated in the previous study carried out in our group with the same molecules can be ascribed to the more severe experimental conditions employed here: the heating temperature was 473 K (compared to 423 K in [26]) and the duration of the heating was extended to 72 h (compared to ca. 5 h in [26]). In particular, Heuberger et al. [26], who studied the effect of the length of the alkyl chain on the chemistry of thermal films and tribofilms formed from alkylated TPPTs at 423 K on air-oxidized 100Cr6 steel discs, pointed out that both thermal films (non-contact region of the discs used for tribological tests) and tribofilms consist of a mixture of phosphates and sulphates. The composition turned out to depend on the chain length: with longer chains the phosphate concentration decreased, while the sulphur concentration increased [26].

### 4.4 Proposed Reaction Mechanism

Based on the findings mentioned above, the reaction mechanism depicted in Scheme 1 is suggested.

As was already observed in the case of TPPT (without any alkyl chain bound to the phenyl rings) [21], at 423 and 473 K the temperature is high enough to start the decomposition of alkylated TPPTs in synthetic oil: the molecules undergo a nucleophilic attack (e.g. by means of OH groups) at the phosphorus atom to cause P=S bond scission to give alkylated triphenyl phosphite. Moreover, since according to the "Principle of Hard and Soft Acids and Basis" (HSAB), thiophosphoryl sulphur is a "soft base" and preferentially reacts with "soft acids", such as tetrahedral carbon [16–19, 59], the alkylation of the sulphur atom can occur (through the isomerization of the molecule, which results in the migration of the alkyl group from the phenyl ring to the sulphur atom). The subsequent breakage of the weak P–S bond results in the formation of volatile compounds (i.e. thiols, where hydrogen is provided by the base oil) and alkylated triphenyl phosphite.

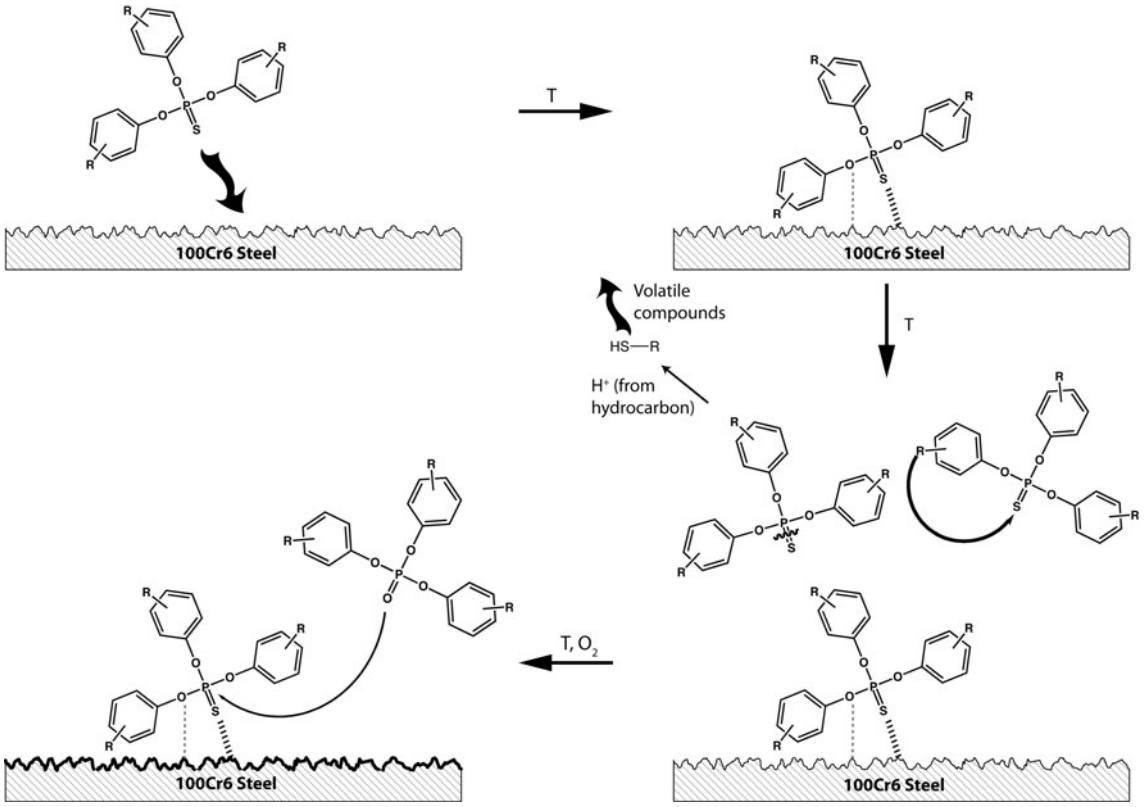


**Scheme 1** Reaction mechanism of alkylated triphenyl phosphorothionates (the alkyl chain R is *t*-butyl (b-TPPT) or *p*-nonyl (n-TPPT)) on 100Cr6 steel surface at 473 K

A thermo-oxidative reaction then takes place, which leads to the oxidation of alkylated triphenyl phosphite to alkylated triphenyl phosphate.

In the case of b-TPPT, no statement can be made about the following reaction step, i.e. the cleavage of the P–O or C–O bond. In contrast, in the case of n-TPPT, since the C–O stretching vibration of the oxidation products of the base oil was found to be superimposed on the *ν*C–O–(P) band at 1169 $cm^{-1}$, the DI of *ν*C–O–(P) band at 1203 $cm^{-1}$ could be calculated, allowing, as a consequence, the identification of the reaction step following the P=S bond scission: the P–O bond turned out to preferentially break over the C–O bond at both 423 and 473 K.

When the heating experiments are performed in the presence of steel filings, the alkylated triphenyl phosphorothionate molecules might adsorb via the sulphur atom to the steel surface, in agreement with Heuberger et al. [25, 26] and as proposed in our previous study in the case of triphenyl phosphorothionate without any substituent attached to the phenyl rings [24]. A polar interaction between the $O_{P–\mathbf{O}–Ph}$ atom and the nascent iron/steel surface cannot be excluded, however, as pointed out by Koyama et al. [27].

The sulphur–metal coordination induces a partial positive charge on the phosphorus atom, making the phosphorus atom itself more open to nucleophilic attack [15]. The phosphoryl oxygen of alkylated triphenyl phosphates, which are produced by the thermo-oxidative reaction of alkylated TPPTs in lubricant oil solution, can carry out a nucleophilic attack on the adsorbed phosphorothionate molecule, leading to the formation of pyro/polyphosphates and sulphur-containing volatile compounds. This also results in a lower concentration of alkylated triphenyl phosphates in the oil solution, which corresponds well with the lower intensity of the signals assigned to these molecules in the FT-IR and NMR spectra of the solutions heated in the presence of steel filings or iron particles ($Fe_{part}$ or $FeOx_{part}$) compared to the solutions heated without filings/particles.

The decrease in intensity of the characteristic signals of alkylated TPPTs in the FT-IR spectra might not only be due to the chemical reaction of these compounds in oil solution. Ribeaud pointed out that the volatilization of these compounds is the main reason for the weight loss of triaryl monothiophosphates during thermogravimetric analyses (TGA) [60]. Even if different experimental conditions have been employed in the present work, some evaporation of alkylated TPPTs cannot be ruled out as a contributing factor in the observed decrease in absorbance of the characteristic vibration bands of alkylated TPPTs.

## 5 Conclusions

The following conclusions can be drawn from the results presented in this work:

(i) Alkylated TPPTs have a strong antioxidant effect on the base oil (poly-α-olefin, PAO) at 423 K. Increasing the length of the alkyl chain bound to the phenyl rings results in a stronger antioxidant effect at 423 K;

(ii) At 473 K, the alkylated TPPT molecules do not inhibit the oxidation of the base oil as effectively as at 423 K. The molecules substituted with an alkyl chain (b-TPPT and n-TPPT) reduce the oxidation of the base oil to a slightly higher extent than the molecule without any alkyl chain bound to the phenyl rings (TPPT);

(iii) The b-TPPT and n-TPPT molecules, being not completely decomposed upon heating at 423 K for 168 h and at 473 K for 72 h, have a high thermal stability even in the presence of metallic and oxidized iron/steel;

(iv) The thermo-oxidative reaction of alkylated TPPTs in oil solution starts with the scission of the P=S bond and leads to the formation of alkylated triphenyl phosphate. The reaction pathway is not dependent on the presence of steel filings/iron particles ($Fe_{part}$ or $FeOx_{part}$) in the lubricant;

(v) The concentration of alkylated triphenyl phosphate present in the oil solution and produced by the thermo-oxidative degradation of alkylated TPPTs is lower when the heating experiments are carried out in the presence of steel filings or iron particles ($Fe_{part}$ or $FeOx_{part}$);

(vi) The kinetics of the thermo-oxidative degradation of alkylated TPPTs is slower when steel filings or iron particles ($Fe_{part}$ or $FeOx_{part}$) are added to the oil solution during the heating experiments;

(vii) At 423 K, the TPPT molecule, not substituted with any alkyl chain, is more reactive than alkylated TPPTs. At 473 K, the reactivity of TPPT and n-TPPT is comparable, but higher than that of b-TPPT. In the case of the experiments performed at 473 K in the presence of steel filings or iron particles ($Fe_{part}$ or $FeOx_{part}$), the reactivity of the alkylated TPPT molecules decreases with the length of the alkyl chain bound to the phenyl rings;

(viii) A reaction layer is formed on the 100Cr6 steel filings immersed in a solution of alkylated TPPTs for 72 h and found to consist of carbon, oxygen, phosphorus and iron. No sulphur was ever detected in the films during the sputter depth profiling.

**Acknowledgements** The authors wish to express their gratitude to the ETH Research Commission for its support of this work. Dr. H. Camenzind (Ciba Speciality Chemicals, Basel, Switzerland) is thanked for supplying the pure additive. Mrs. D. Sutter and Mr. M. Schneider kindly performed the NMR and the elemental analysis, respectively.

## References

1. Kubsh, J.: Three-way catalyst deactivation associated with oil-derived poisons. In: Bode, H. (ed.) Materials Aspects in Automotive Catalytic Converters, pp. 215–222. Wiley-VCH Verlag GmbH & Co, Weinheim (2003)
2. Mang, T., Dresel, W. (eds.): Lubricants and Lubrication, p. 850. Wiley, New York (2007)
3. Rudnick, L.R. (ed.): Lubricant Additives: Chemistry and Applications, p. 790. Marcel Dekker Inc, New York (2003)
4. Gellman, A.J., Spencer, N.D.: Surface chemistry in tribology. J. Eng. Tribol. **216**(6), 443–461 (2002)
5. Nicholls, M.A., Do, T., Norton, P.R., Kasrai, M., Bancroft, G.M.: Review of the lubrication of metallic surfaces by zinc dialkyldithiophosphates. Tribol. Int. **38**(1), 15–39 (2005)
6. Spikes, H.A.: The history and mechanisms of ZDDP. Tribol. Lett. **17**(3), 469–489 (2004)
7. McDonald, R.A.: Zinc dithiophosphates. In: Rudnick, L.R. (ed.) Lubricant Additives: Chemistry and Applications, pp. 29–43. Marcel Dekker, New York (2003)
8. Rasberger, M.: Oxidative degradation and stabilization of mineral oil based lubricants. In: Mortier, R.M., Orszulik, S.T. (eds.) Chemistry and Technology of Lubricants, pp. 98–143. Blackie Academic & Professional, London (1997)
9. Willermet, P.A., Carter, R.O., Schmitz, P.J., Everson, M., Scholl, D.J., Weber, W.H.: Formation, structure, and properties of lubricant-derived antiwear films. Lubr. Sci. **9**(4), 325–348 (1997)
10. Jones, R.B., Coy, R.C.: The chemistry and thermal degradation of zinc dialkyldithiophosphate additives. ASLE Trans. **24**(1), 91–97 (1981)
11. Olree, R.M., McMillan, M.L.: How Much ZDP is Enough? SAE Technical Papers, 2004 (Paper No. 2004-01-2986)
12. Spikes, H.A.: Low- and zero-sulphated ash, phosphorus and sulphur anti-wear additives for engine oils. Lubr. Sci. **20**(2), 103–136 (2008)
13. Spikes, H.A.: Beyond ZDDP. Lubr. Sci. **20**(2), 77–78 (2008)
14. Hilgetag, G., Teichmann, H.: The alkylating properties of alkyl thiophosphates. Angew. Chem. Int. Ed. **4**(11), 914–922 (1965)
15. Teichmann, H., Hilgetag, G.: Nucleophilic reactivity of the thiophosphoryl group. Angew. Chem. Int. Ed. **6**(12), 1013–1023 (1967)
16. Pearson, R.G.: Hard and Soft Acids and Bases, p. 480. Dowden Hutchinson & Ross, Stroudsburg, PA (1973)
17. Pearson, R.G.: Chemical Hardness, p. 198. Wiley, New York (1997)
18. Pearson, R.G.: Hard and soft acids and bases. J. Am. Chem. Soc. **85**(22), 3533–3539 (1963)
19. Pearson, R.G.: Hard and soft acids and bases, HSAB, Part I, fundamental principles. J. Chem. Educ. **45**(9), 581–586 (1968)
20. Rossi, A., Piras, F.M., Kim, D., Gellman, A.J., Spencer, N.D.: Surface reactivity of tributyl thiophosphate: effects of temperature and mechanical stress. Tribol. Lett. **23**(3), 197–208 (2006)
21. Mangolini, F., Rossi, A., Spencer, N.D.: Reactivity of triphenyl phosphorothionate in lubricant oil solution. Tribol. Lett. **35**(1), 31–43 (2009)

22. Braun, J.: Additives. In: Mang, T., Dresel, W. (eds.) Lubricants and Lubrication, pp. 88–118. Wiley, New York (2007)
23. Migdal, C.A.: Antioxidants. In: Rudnick, L.R. (ed.) Lubricant Additives: Chemistry and Applications, pp. 1–27. Marcel Dekker, New York (2003)
24. Mangolini, F., Rossi, A., Spencer, N.D.: Influence of metallic and oxidized iron/steel on the reactivity of triphenyl phosphorothionate in oil solution. Tribol. Int. (2010). (in press)
25. Heuberger, R.: Combinatorial study of the tribochemistry of antiwear lubricant additives. PhD Thesis no. 17207, ETH Zurich, Zurich, Switzerland (2007)
26. Heuberger, R., Rossi, A., Spencer, N.D.: Reactivity of alkylated phosphorothionates with steel: a tribological and surface-analytical study. Lubr. Sci. **20**(2), 79–102 (2008)
27. Koyama, M., Hoyakawa, J., Onodera, T., Ito, K., Tsuboi, H., Endou, A., Kubo, M., DelCarpio, C.A., Miyamoto, A.: Tribochemical reaction dynamics of phosphoric ester lubricant additive by using a hybrid tight-binding quantum chemical molecular dynamics method. J. Phys. Chem. B **110**(35), 17507–17511 (2006)
28. Additive Data Sheets, Ciba Speciality Chemicals. Basel, Switzerland (2003)
29. Vogel, I., Svehla, G.: Textbook of Macro and Semimicro Qualitative Inorganic Analysis, p. 605. Longman, New York (1979)
30. Socrates, G.: Infrared and Raman Characteristic Group Frequencies, p. 347. Wiley, Chichester (2001)
31. Harris, R.K., Becker, E.D., Cabral De Menezes, S.M., Goodfellow, R., Granger, P.: NMR Nomenclature. Nuclear spin properties and conventions for chemical shifts. Pure Appl. Chem. **73**(11), 1795–1818 (2001)
32. Scofield, J.H.: Hartree-Slater subshell photoionization cross-sections at 1254 and 1487 eV. J. Electron Spectrosc. Relat. Phenom. **8**(2), 129–137 (1976)
33. Reilman, R.F., Msezane, A., Manson, S.T.: Relative intensities in photoelectron spectroscopy of atoms and molecules. J. Electron Spectrosc. Relat. Phenom. **8**(5), 389–394 (1976)
34. Briggs, D., Grant, J.T. (eds.): Surface Analysis by Auger and X-Ray Photoelectron Spectroscopy, p. 899. IM Publications, Chichester (2003)
35. Seah, M.P., Dench, W.A.: Quantitative electron spectroscopy of surfaces: a standard data base for electron inelastic mean free paths in solids. Surf. Interface Anal. **1**(1), 2–11 (1979)
36. Bellamy, L.J.: The Infra-red Spectra of Complex Molecules, p. 433. Chapman and Hall, London (1975)
37. Lin-Vien, D., Colthup, N.B., Fateley, W.G., Grasselli, J.G.: The Handbook of Infrared and Raman Characteristic Frequencies of Organic Molecules, p. 503. Academic Press, San Diego (1991)
38. Roeges, N.P.G.: A Guide to the Complete Interpretation of Infrared Spectra of Organic Structures, p. 340. Wiley, Chichester (1994)
39. Silverstein, R.M., Webster, F.X., Kiemle, D.J.: Spectroscopic Identification of Organic Compounds, p. 502. Wiley, New York (2005)
40. Thomas, L.C.: The identification of functional groups in organophosphorus compounds. In: Belcher, R., Anderson, D.M.W. (eds.) The Analysis of Organic Materials, vol. 7, p. 121. Academic Press, London (1974)
41. Chittenden, R.A., Thomas, L.C.: Characteristic infra-red absorption frequencies of organophosphorus compounds—III. Phosphorus-sulphur and phosphorus-selenium bonds. Spectrochim. Acta **20**(11), 1679–1696 (1964)
42. Thomas, L.C., Chittenden, R.A.: Characteristic infrared absorption frequencies of organophosphorus compounds—II. P–O–(X) bonds. Spectrochim. Acta **20**(3), 489–502 (1964)
43. Friebolin, H.: Basic One- and Two-Dimensional NMR Spectroscopy, p. 430. Wiley, New York (2005)
44. Günther, H.: NMR Spectroscopy - Basic Principles, Concepts, and Applications in Chemistry, p. 581. Wiley, New York (1995)
45. Hesse, M., Meier, H., Zeeh, B.: Spektroskopische Methoden in der Organischen Chemie, 3. überarbeitete Auflage. Georg Thieme Verlag Stuttgart, New York (1987)
46. Berger, S., Braun, S., Kalinowski, H.-O.: NMR Spectroscopy of the Non-metallic Elements. Wiley, New York (1997). 1082
47. Crutchfield, M.M., Dugan, C.H., Letcher, J.H., Mark, V., Van Wazer, J.R.: P31 nuclear magnetic resonance. In: Grayson, M., Griffith, E.J. (eds.) Topics in Phophorus Chemistry, vol. 5, p. 492. Wiley, New York (1967)
48. Quin, L.D.: A Guide to Organophosphorus Chemistry, p. 408. Wiley, New York (2000)
49. Colthup, N.B., Daly, L.H., Wiberley, S.E.: Introduction to Infrared and Raman Spectroscopy, p. 547. Academic Press, London (1990)
50. Adhvaryu, A., Perez, J.M., Singh, I.D., Tyagi, O.S.: Spectroscopic studies of oxidative degradation of base oils. Energy Fuels **12**(6), 1369–1374 (1998)
51. Eglin, M., Rossi, A., Spencer, N.D.: X-ray photoelectron spectroscopy analysis of tribostressed samples in the presence of ZnDTP: a combinatorial approach. Tribol. Lett. **15**(3), 199–209 (2003)
52. Onyiriuka, E.C.: Zinc phosphate glass surfaces studied by XPS. J. Non-Cryst. Solids **163**(3), 268–273 (1993)
53. Coates, J.P., Setti, L.C.: Infrared spectroscopic methods for the study of lubricant oxidation products. ASLE Trans. **29**(3), 394–401 (1986)
54. Coy, R.C., Jones, R.B.: The thermal degradation and ep performance of zinc dialkyldithiophosphate additives in white oil. ASLE Trans. **24**(1), 77–90 (1981)
55. Dickert, J.J.J., Rowe, C.N.: The thermal decomposition of metal O,O-dialkylphosphorodithioates. J. Org. Chem. **32**(3), 647–653 (1967)
56. Spedding, H., Watkins, R.C.: The antiwear mechanism of ZDDP'S Part I. Tribol. Int. **15**(1), 9–12 (1982)
57. Mortimer, F.S.: Vibrational assignment and rotational isomerism in some simple organic phosphates. Spectrochim. Acta **9**(4), 270–281 (1957)
58. Hernandez, J., Goycoolea, F.M., Zepeda-Rivera, D., Juarez-Onofre, J., Martunez, K., Lizardi, J., Salas-Reyes, M., Gordillo, B., Velazquez-Contreras, C., Garcia-Barradas, O., Cruz-Sanchez, S., Dominguez, Z.: Substituent effects on the 31P NMR chemical shifts of arylphosphorothionates. Tetrahedron **62**(11), 2520–2528 (2006)
59. Pearson, R.G., Songstad, J.: Application of the principle of hard and soft acids and bases to organic chemistry. J. Am. Chem. Soc. **89**(8), 1827–1836 (1967)
60. Ribeaud, M.: Volatility of phosphorus-containing anti-wear agents for motor oils. Lubr. Sci. **18**(3), 231–241 (2006)